J Appl Physiol 126: 1360–1376, 2019.
First published March 7, 2019; doi:10.1152/japplphysiol.00166.2018.

REVIEW | *Cores of Reproducibility in Physiology*

Understanding near infrared spectroscopy and its application to skeletal muscle research

Thomas J. Barstow

Department of Kinesiology, Kansas State University, Manhattan, Kansas

Submitted 16 February 2018; accepted in final form 4 February 2019

Barstow TJ. Understanding near infrared spectroscopy and its application to skeletal muscle research. *J Appl Physiol* 126: 1360–1376, 2019. First published March 7, 2019; doi:10.1152/japplphysiol.00166.2018.—Near infrared spectroscopy (NIRS) is a powerful noninvasive tool with which to study the matching of oxygen delivery to oxygen utilization and the number of new publications utilizing this technique has increased exponentially in the last 20 yr. By measuring the state of oxygenation of the primary heme compounds in skeletal muscle (hemoglobin and myoglobin), greater understanding of the underlying control mechanisms that couple perfusive and diffusive oxygen delivery to oxidative metabolism can be gained from the laboratory to the athletic field to the intensive care unit or emergency room. However, the field of NIRS has been complicated by the diversity of instrumentation, the inherent limitations of some of these technologies, the associated diversity of terminology, and a general lack of standardization of protocols. This Cores of Reproducibility in Physiology (CORP) will describe in basic but important detail the most common methodologies of NIRS, their strengths and limitations, and discuss some of the potential confounding factors that can affect the quality and reproducibility of NIRS data. Recommendations are provided to reduce the variability and errors in data collection, analysis, and interpretation. The goal of this CORP is to provide readers with a greater understanding of the methodology, limitations, and best practices so as to improve the reproducibility of NIRS research in skeletal muscle.

absorption; adipose tissue thickness; blood flow; oxygen utilization; scattering

INTRODUCTION

The application of near infrared spectroscopy (NIRS) to study physiology has increased exponentially in recent years, with PubMed listing over 1,150 citations for the application to "exercise," 800 for "ischemia," and 5,200 for "cerebral." The number of studies speaks to the extensive interest in, applications of, and literature on this technology. Given the extent of the literature, not every relevant study could be cited in this Cores of Reproducibility in Physiology (CORP). This CORP will provide an overview of the multitude of NIRS technologies, their applications to skeletal muscle at rest and during exercise, and the important considerations when designing experiments and interpreting data so as to improve the accuracy and reproducibility of the resulting NIRS data. Although the author has attempted to provide generally accepted information and suggestions, it should be recognized that this CORP is not a consensus statement from a group of NIRS users but the recommendations of one individual.

Address for reprint requests and other correspondence: T. J. Barstow, Dept. of Kinesiology, Kansas State University, 8 Natatorium, 920 Denison Ave, Manhattan, KS 66506 (e-mail: tbarsto@ksu.edu).

In any tissue undergoing aerobic metabolism, adequate delivery of oxygen ($\dot{Q}O_2$) to meet the metabolic demands ($\dot{V}O_2$) is critical for long-term viability of that tissue. Delivery of oxygen to the terminal cytochrome oxidase ($cyto_{ox}$) can be described by the integration of two equations first delineated by Adolph Fick (58): perfusive (Fick equation, *Eq. 1*) and diffusive (Fick's Law of Diffusion, *Eq. 2*) (59) O_2 delivery (Fig. 1).

$$\dot{V}_{O_2} = \dot{Q} \cdot \left(C_a - C_v\right)O_2 \qquad (1)$$

$$\dot{V}_{O_2} = D_{O_2} \cdot \left(PmvO_2 - PmitoO_2\right) \qquad (2)$$

where $\dot{Q}$ is blood flow; Ca and Cv are O_2 concentrations in arterial and venous blood, respectively; DO_2 is the diffusivity of O_2; and $PmvO_2$ and $PmitoO_2$ are the partial pressures of O_2 in the microvasculature and mitochondria, respectively.

Due to the positive intercept on the $\dot{Q}/\dot{V}O_2$ relationship, venous PvO_2 and CvO_2 coming from skeletal muscle are predicted to fall [and the $(a - v)O_2$ difference rise] with increasing metabolic rate (as $\dot{V}O_2$) (55). In addition, Fick's Law of Diffusion also predicts that increases in tissue $\dot{V}O_2$ are accomplished in part by widening of the microvascular-tissue PO_2 gradient (i.e., PO_2 at $cyto_{ox}$ falls) to facilitate increases in O_2 diffusion. The responses of both Fick equations provide insight into, and are significantly determined by, the relative balance between $\dot{Q}O_2$

8750-7587/19 Copyright © 2019 the American Physiological Society

Downloaded from journals.physiology.org/journal/jappl (065.021.193.086) on March 4, 2022.

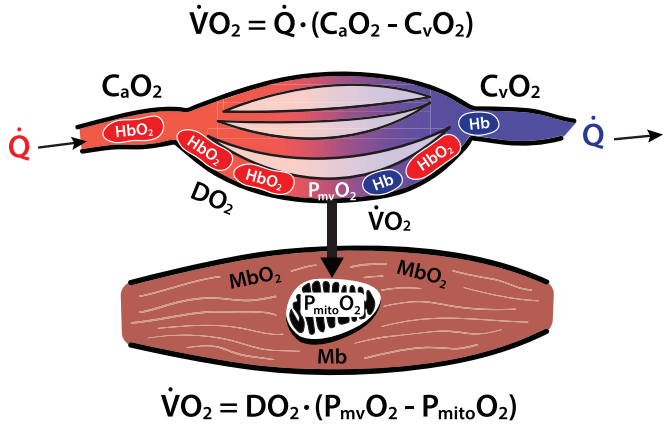

Fig. 1. Schematic showing components of oxygen delivery (through the Fick Equation, *top*) and oxygen diffusion from capillary to muscle fiber mitochondria (Fick's Law of Diffusion, *bottom*). Ca_{O_2}, arterial concentration of O_2; Cv_{O_2}, venous content of O_2 draining the muscle/limb; Do_2, diffusivity of O_2; Mb, myoglobin; $PmitoO_2$, mitochondrial partial pressure of O_2; $PmvO_2$, microvascular partial pressure of O_2; $\dot{Q}$, blood flow; $\dot{V}o_2$, oxygen uptake.

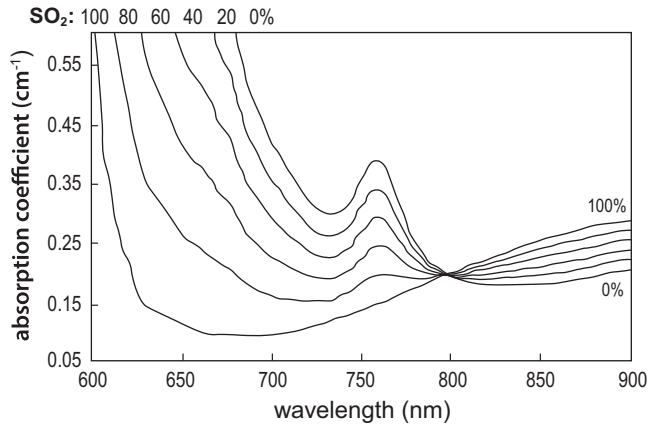

Fig. 2. Near infrared (NIR) absorption spectra of hemoglobin at various saturations from 0% to 100% across the range of near infrared spectra. Note that in the NIR range the spectra for myoglobin and hemoglobin are almost superimposable. [Redrawn with permission from (63).]

and $\dot{V}o_2$ to skeletal muscle. To determine this balance in humans typically requires invasive and/or expensive techniques [e.g., MRI/MRS, PET, arterial/venous catheterization) (22)] when possible, but often is problematic depending on the tissue/organ of interest. A noninvasive methodology for determining relative or absolute global tissue oxygenation would thus be invaluable, especially in protocols where repeated measurements are required and/or in patients where testing opportunities are limited. Near-infrared spectroscopy (NIRS) provides just such noninvasive methodology. It should be appreciated, however, that noninvasive monitoring of muscle oxygenation using NIRS presents several challenges, including the presence of tissues (skin with varying concentration of melanin, adipose tissue) which lie between the surface and the muscle(s) of interest. Complex tissue arrangements, including the dimensions of muscles, presence of large blood vessels, and even bone can affect the NIRS signals. Furthermore, muscle will often change its shape/configuration during contraction, which can alter the scattering of light traveling through the tissues. Sections of this CORP will discuss some of these potential complications and provide recommendations when appropriate or possible.

NIRS can be used to determine the concentration and oxygenation status of light-absorbing chromophores in biological tissues. Unlike visible light (~400–650 nm), where the shorter wavelengths are unable to penetrate into tissues, light in the near infrared (NIR) (3) region (~700–900 nm) is potentially able to penetrate several millimeters or more into biological tissues, where the main absorbing chromophores in skeletal muscle are hemoglobin (Hb), myoglobin (Mb), and cytochrome oxidase (cyt_{ox}). (note, at longer wavelengths within this region, both water and fat exhibit large absorption peaks). Hemoglobin and myoglobin contain an iron core within each heme, which varies its light absorption in the NIR range based on whether or not oxygen is bound to it (Fig. 2). In contrast, cyt_{ox} contains four redox centers: two hemes (known collectively as aa_3) and two copper sites. Electrons pass between these centers in a series of redox reactions producing associated optical changes. In the NIR region, the Cu-Cu dimer copper A (CuA) dominates the absorption spectrum, which when oxidized produces a strong peak around 830 to 840 nm (4). However, the concentration of cyt_{ox} in mammalian muscle is likely ~5% or less compared with that of hemoglobin and myoglobin (3, 34), suggesting the primary sources of the NIRS signals are hemoglobin and myoglobin heme. The relative signal strengths of the hemoglobin and myoglobin result in 4 basic NIRS variables that could potentially be determined, depending on the technology utilized (see below)—oxy[Hb+Mb], deoxy[Hb+Mb], total[Hb+Mb] (which is the sum of oxy- and deoxy[Hb+Mb]), and tissue saturation (as oxy[Hb+Mb]/total[Hb+Mb]). Deoxy[Hb+Mb] has been viewed as a proxy variable for the perfusive term in *Eq. 1* [(Ca – Cv)O_2] (39, 67), while changes in total[Hb+Mb], reflecting changes in capillary hematocrit (34), have been interpreted as an indicator of the diffusive term Do_2 in *Eq. 2*. A note on standardization is in order here. The field of application of NIRS to study brain and muscle physiology has engendered several redundant terms for both the 4 basic NIRS variables above and for certain protocols. Table 1 provides the terms chosen for this CORP, along with the equivalent terms used elsewhere. We strongly encourage all investigators using NIRS in the future to adopt the standard of referring to oxygenated, deoxygenated, and total [heme], as this reflects the fundamental source(s) of the NIRS signals, irrespective of relative contributions of [Hb] or [Mb]. Hopefully the rationale for this will become apparent later in the CORP.

Jöbsis (81) was the first to apply NIRS to monitor heart muscle and cerebral oxygenation in situ and in vivo, respec-

Table 1. *Nomenclature frequently used in NIRS studies*

Used in this Paper*	Other Common Equivalent Terms*
total[heme]*	total[Hb+Mb]; [tHb]
oxy[heme]*	oxy[Hb+Mb]; O_2Hb; HbO_2
deoxy[heme]*	deoxy[Hb+Mb]; HHb
StO_2, %	Muscle tissue oxygen saturation (SmO_2); Tissue Oxygenation Index (TOI); Tissue Saturation Index (TSI)

Hb, hemoglobin; Mb, myoglobin. *Units depend on specific instrument used.

Downloaded from journals.physiology.org/journal/jappl (065.021.193.086) on March 4, 2022.

tively. According to the Beer-Lambert law, the attenuation of light in a nonscattering medium is given by

$$A(OD) = log(I_o/I) = \varepsilon \cdot [C] \cdot L \quad (3)$$

where A is light attenuation; I_o, incident (source) light; I, emergent light; ε, specific extinction coefficient; [C], chromophore concentration (e.g., [Hb], [Mb], and/or [cyt_{ox}]); and L, light path length (distance between points where light enters and leaves the medium, i.e., source-detector separation) (Fig. 3*A*).

SIGNIFICANCE OF SCATTERING

However, biological tissues are highly scattering media and scattering will increase the path length of light, increasing the probability of both light absorption and loss of light (Fig. 3*B*, *lines 3, 4*). Light scattering is a complex process occurring when photons cross membrane boundaries (cell and intracellular organelle) due to the changes in the refractive index of the various media (123). The Beer-Lambert law was subsequently modified to account for these effects on light attenuation (40, 123)

$$A = log(I_o/I) = \varepsilon \cdot [C] \cdot L \cdot DPF + G \quad (4)$$

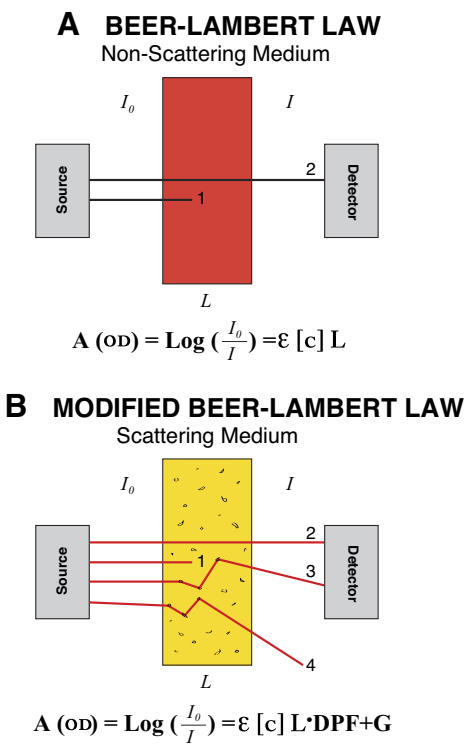

Fig. 3. Schematics demonstrating the original Beer-Lambert Law (*A*) for a nonscattering solution and the subsequent modified Beer-Lambert Law (*B*) to account for scattering in biological tissues. A, absorption; [C] concentration of compound of interest; DPF, differential path length factor; ε, extinction coefficient for the light absorbing compound of interest; G, factor reflecting non-absorption loss of photons; 4, loss of photons from field of view due to scattering, but not absorption (G in Modified Beer-Lambert equation); I_o, source light intensity; I, detected light; L, source-detector distance. 1, loss of photons due to absorption; 2, photons that are not absorbed and travel a nonscattering path length (source-detector distance L) to be recorded by detector; 3, photons that are not absorbed but are scattered on their way to the detector, increasing their path length by L*DPF.

where the differential path length factor (DPF) is included to account for the extended path length due to scattering, and G represents losses due to scattering. DPF is estimated as the mean path length from the temporal point spread function determined from time-of-flight (ToF) measurements divided by the source-detector separation (41), i.e., it represents a multiplicative correction factor (e.g., a DPF of 4 means the mean path length of photons in the tissue is 4 times the source-detector separation). The extinction coefficient ε varies with both wavelength and heme oxygenation status. As the interrogating wavelength gets longer (e.g., from 750 to 840 nm), ε for deoxy[Hb+Mb] decreases, but ε for oxy[Hb+Mb] gets larger (84). Since longer wavelengths will penetrate deeper into the tissue, it is presently unclear if differences in depth of penetration, combined with the different responses of ε as a function of wavelength, are sufficiently different for short (~690 nm) versus longer (e.g., ~830 nm) wavelengths as to negate the assumption that spectral information from more than one wavelength arises from the same tissue depth/volume. See further discussion below under *Cutaneous Blood Volume/Flow*.

It is important to note that the DPF is not a constant value but varies for several reasons (41). *1*) There is variability in the time of flight of photons through a scattering medium such as biological tissue; the DPF is calculated as the mean of this dispersion of values. (Note, the time of flight method has historically been considered the gold standard for quantifying NIRS signals in biological tissues). The first occurrence of the term DPF appears to have been in experiments in the rat skull/brain, where the mean ± SD DPF was found to be 5.3 ± 0.3 times the diameter of the skull (i.e., the source-detector separation) (41). It is important to note that the 5% to 95% values ranged from 2.6 to 9.2, illustrating the range of relative photon path lengths. Thus, even the gold standard has variability inherent in its measurement. *2*) The DPF also represents the instantaneous slope of the plot of attenuation versus absorption ($\delta OD/\delta\mu_a$), which is not linear but depends on both absorption and scattering coefficients. *3*) DPF increases with increasing scattering and decreases with increasing absorption. This can be seen by the relationship between DPF and both absorption (μ_a) and reduced scattering (μ_s') coefficients (53):

$$DPF = \frac{\sqrt{3\mu_s'}}{2\sqrt{\mu_a}}$$

4) Generally, scattering decreases with increasing wavelength (41, 46, 53). 5) There is appreciable intersubject variation in DPF at rest. This variability for wavelengths of 690 nm to 832 nm extends to site [gastrocnemius (5.8 to 5.3) versus forearm (4.4 to 3.9) versus adult head (6.5 to 5.9) versus infant head (5.4 to 4.7)], with women having greater DPF than men for the forearm and calf muscle (46, 51). Intersubject coefficients of variation (SD* 100/mean) typically ranged from 16 to 20% for muscle sites and 9 to 17% for the brain. Similar values of DPF for the vastus lateralis were found by Ferreira et al. (53) for both mean (4.27 to 5.22 for 690 nm and 830 nm) and CV (17–19%) at rest. This variation reinforces caution regarding the use of a single common value for DPF across subjects and tissue sites. 6) The DPF can vary with venous occlusion and muscle contractions, two procedures commonly utilized with NIRS (51). It is currently unclear how significant these potential errors in quantification of the NIRS responses could be. For

Downloaded from journals.physiology.org/journal/jappl (065.021.193.086) on March 4, 2022.

example, in protocols where subjects act as their own controls, would this reduce the qualitative significant of assuming scattering and/or DPF to remain constant? Future work should examine if clinical interpretation, prognosis, and decisions based on continuous wave NIRS responses would be altered if scattering were measured.

Ferreira et al. (53) used a frequency domain multidistance (FDMD) system (see below), which permitted continuous measurement of μ_s', to determine the intersubject variability of scattering (μ_s') and DPF at rest and during incremental exercise. They found *1*) there was considerable intersubject variability in μ_{s690}' and μ_{s830}', and thus DPF, measured in the quadriceps at rest. *2*) The DPF was different for 690 versus 830 nm (DPF: 690 nm 5.22 ± 0.88; 830 nm 4.49 ± 0.83). *3*) DPF_{690} and DPF_{830} fell significantly (6.8% and 5.0%, respectively) during incremental cycling exercise. *4*) Assuming constant μ_s' led to an overestimation of changes in [deoxy(Hb+Mb)] (63%), [oxy(Hb+Mb)] (134%), and StO_2 (58%) especially at moderate to heavy exercise intensities. *5*) The kinetics of [deoxy(Hb+Mb)] during recovery from incremental exercise were significantly slower when μ_s' was assumed constant. Since with most commercial NIRS systems it is not possible to determine a priori the actual value of DPF or μ_s' for a given subject, nor which subjects will demonstrate changes in μ_s' and DPF during interventions like occlusion, cuff release, and exercise, the assumption of constant μ_s' and DPF is invalid. Therefore, if mechanistic insights are to be gained from investigation of physiologically relevant NIRS variables, μ_s' and DPF cannot be assumed to be the same for all subjects nor to remain constant during interventions like dynamic exercise or postocclusive reactive hyperemia (PORH) or vascular occlusion test (VOT) experiments. Importantly, quantitative measurements of [c] (e.g., oxy- and deoxy[Hb+Mb] in a scattering medium) cannot be made without knowledge of DPF and G. However, it should be noted that by using the modified Lambert-Beer law, CW NIRS instruments can provide changes in the concentrations of oxy[heme] and deoxy[heme] with respect to an initial baseline value arbitrarily set to zero in units of micromoles per centimeter.

In vitro, changes in total[Hb+Mb] are associated with parallel changes in μ_s'. Thus increases in total[Hb+Mb], often seen during cuff occlusion and exercise, may produce increases in scattering (μ_s') (26, 49, 53, 67). Any changes in the water content will modify the tissue refractive index and consequently the μ_s'. Skeletal muscle water content is typically assumed to be 75% of the total volume and constant across acute interventions (60). However, exercise can lead to significant increases in tissue water (62). The effect of this assumption on the NIRS signal is unknown; In addition, the increase in muscle temperature during exercise (91) will produce changes in the water and lipids spectra; however, it is unclear how the ~1–2°C increase in muscle temperature with heavy exercise (92) will quantitatively affect the results of NIRS measurements of muscle oxygenation.

NIRS TECHNOLOGIES

There are three broad categories of NIRS oximeters that have been used to measure muscle oxygenation (oximetry): continuous wave (CW), time-resolved (TRS) or time domain (TD) or time of flight, and frequency domain (FD) intensity-modulated (40, 135) (Fig. 4). (See section below for discussion of the latest technologies.)

Continuous Wave

The earliest, and still most common due to their relatively inexpensive cost, commercial instruments were continuous wave (CW) near-infrared spectrometers (26), where the light source is of constant intensity and the transmitted light intensity is detected, providing only changes in light attenuation. The implicit assumption is made that DPF and G (and thus μ_s') are always constant, so that changes in the light attenuation (ΔA) from an arbitrary baseline then reflect changes in concentration (Δ[c]). Output variables typically are a "difference signal," representing tissue deoxygenation and a "blood volume" signal, reflecting total signal strength (total[Hb+Mb]). An improvement to the original one source-detector pair is the spatially-resolved spectrometers (SRS) (134), where photons are measured at multiple spacings from the source, improving the precision of the estimation of (ε·[C]·L) in *Eq. 2*. In addition, the SRS system design enhances contribution of deeper tissues, while reducing contribution of more superficial tissue like skin/adipose tissue, to the NIRS signals (105). SRS systems typically provide a quantitative measure of tissue oxygenation with one or more synonymous terms: muscle tissue oxygen saturation (SmO_2), tissue oxygen saturation (StO_2), tissue oxygenation index (TOI), or tissue saturation index (TSI), all calculated as oxy[heme]*100/total[Heme] and expressed as percent (4, 68, 129). It is important to appreciate that CW

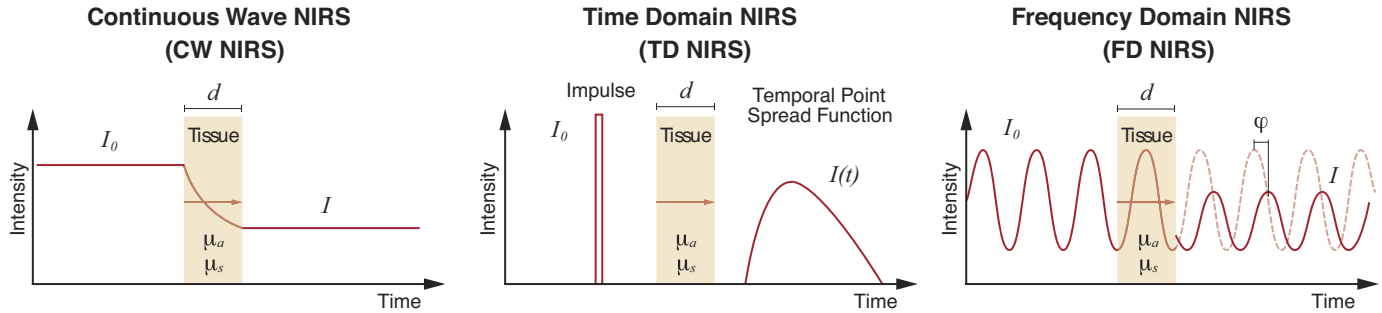

Fig. 4. Schematic showing the three main types of near infrared (NIR) instruments. d, source-detector separation (L in *Eqs. 3–5*). Phase shift (ϕ) used to determine μ_a and μ_s'. See text for more details. FD, frequency domain; I_o, source light intensity; *I*, detected light; TD, time domain. [Redrawn with permission from (40, 129).]

Downloaded from journals.physiology.org/journal/jappl (065.021.193.086) on March 4, 2022.

spectrometers, including SRS, do not provide absolute concentrations of chromophores in the interrogated tissues because the actual path length of light (L·DPF) is unknown. As noted above, however, changes in the concentrations of oxy[heme] and deoxy[heme] with respect to an initial baseline value can be determined by SRS instruments.

Time Domain or Time Resolved Spectroscopy

TD or TRS NIRS employs a pulsed light source, typically a laser providing light pulses with duration of a few tens of picoseconds, and a detection apparatus with temporal resolution in the subnanosecond scale (41). The photon distribution of the resulting time-of-flight (DTOF) or temporal point spread function (TPSF) is then measured at a fixed distance from the injection point (source-detector separation typically in the range of 10–40 mm). Due to scattering in the tissues, the resulting signal is delayed (reflecting time of travel from source to detector), broadened (due to the multitude of path lengths of the photons as they are scattered), and attenuated (because absorption reduces the probability of detecting a photon) (135). This detection-time curve is fitted to resolve the absorption coefficient (μ_a), the reduced scattering coefficient (μ_s'), and the mean path length (PL; calculated from the measured mean time of flight), by application of diffusion theory (114, 115). Knowledge of these three variables permits calculation of absolute deoxy[Hb+Mb], oxy[Hb+Mb], and their sum, total[Hb+Mb] in micromolar units. A recent advance in data processing of TD signals permitted discrimination of the relative contribution of signals coming from upper layers of the tissue from those originating in deeper layers, using information on the photon path length (121).

Frequency Domain

FD NIRS is based on amplitude-modulated light sources (at a frequency of the order of 100 MHz or larger). One of these techniques, frequency-domain multi-distance (FDMD) spectroscopy, determines the average value (dc), amplitude (ac), and phase (ϕ) of the modulated light intensity at several source-detector distances, which by using equations derived from diffusion theory (70, 80), allows for continuous measurement of μ_a and μ_s' for each wavelength used. From these, absolute measurements of the oxygenated and deoxygenated chromophores present in the tissues (deoxy[Hb+Mb], oxy[Hb+Mb], and their sum, total[Hb+Mb] in micromolar units) can be calculated and expressed in micromoles, using the Beer-Lambert law (*Eq. 1*) directly. While the theory underlying the measurements of μ_a and μ_s' by frequency-domain spectroscopy is different from that presented above for continuous-wave spectroscopy (40, 70), the FD measurements can be related to attenuation of light in biological tissues described in *Eqs. 3* and *4* as follows

$$A = ln\left(I_o/I\right) = (m_a + m_s) \cdot L \cdot DPF \qquad (5)$$

where $\mu_s' = (1 - g)\cdot\mu_s$; μ_s is the scattering coefficient and g is the mean cosine of the scattering angle [for more details see (80, 123)].

The accuracy of FD NIRS relies on the validity of assumptions about the tissue optical characteristics made to derive μ_a and μ_s'. These assumptions are that the tissue is macroscopically homogeneous, scatters isotropically, and $\mu_s' \gg \mu_a$. The tissue macroscopic homogeneity is certainly not true for in vivo measurements due to the skin-fat layer separating the NIRS probe from the muscle (main source of changes in μ_a). The superficial layer has major effects on the light intensity (used in single-distance CW methods), while the slopes of average value (dc), amplitude (ac), and phase (ϕ) used to determine μ_a and μ_s' in the FDMD technique are much less affected in a two-layer model (64). To conclude this section, both TD/TRS and FD spectrometers provide absolute concentrations of the heme components in tissue, whereas CW instruments can only provide changes in concentration from an arbitrary baseline and/or StO_2 (68).

SOURCES OF THE NIRS SIGNAL

In skeletal muscle, the primary heme compounds are vascular hemoglobin ([Hb]) and intracellular myoglobin ([Mb]) and cytochrome oxidase (cyt_{ox}). The relative concentration of cyt_{ox} (or cytochrome aa_3) is quantitatively small, being an order of magnitude smaller than [Hb] and [Mb] (44), and thus its contribution to the NIRS signals is typically ignored. Thus this discussion will focus on [Hb] and [Mb]. However, it should be recognized that the total NIRS signal strength (sometimes referred to as total[Hb+Mb]) reflects the concentration of total heme in the field of view.

The actual tissue value for the total[Hb + Mb] in a given skeletal muscle depends on the [Hb] within the muscle microvasculature and the [Mb] of the interrogated muscle. The relative contribution of microvascular [Hb] and intracellular [Mb] to total[Hb + Mb] has been debated for several years, with early investigations concluding that a majority of the NIRS signal originated from [Hb] (98, 130). This conclusion was based on studies using a continuous wave spectrometer, which was not capable of providing quantitative values (98), or on studies performed in a perfused rat hind limb model, where the muscles examined have much lower [Mb] (130) than human muscles (28, 34). More recent work using quantitative NIRS instruments and protocols (8, 99, 136) or morphometric modeling (34) have concluded that [Mb] likely contributes 60–90% to the NIRS signals coming from skeletal muscle. Average values for [Mb] in human skeletal muscle range from ~300 to 700 μM, with Type I fibers reported to have more [Mb] than Type II fibers (6, 113, 138).

The tissue [Hb] contribution to the NIRS signal is a function of the tissue microvascular volume and the microvascular hematocrit (Hct). It is typically stated that the [Hb] signal originates in blood vessels <1 mm in diameter (32) due to almost complete absorption of light in large vessels where [Hb] is locally very high. Based on observations made in exteriorized muscle preparations (with intact vasculature and neural pathways), capillary Hct (reflecting [Hb]) at rest is much lower (12–22%) than systemic Hct (40–45%) (85, 86). Since it is a reasonable assumption that intracellular [Mb] remains constant during acute interventions such as exercise or ischemia-reperfusion (14), changes in total[Hb+Mb] can be attributed to changes in microvascular Hct [for a more detailed discussion of this topic, see (34)]. However, at present, there is no technique for determining microvascular Hct in human skeletal muscle, either at rest or during interventions like exercise or ischemia-reperfusion. This uncertainty in the actual value for resting micro-

Downloaded from journals.physiology.org/journal/jappl (065.021.193.086) on March 4, 2022.

vascular Hct contributes to the intersubject variability in total[Hb + Mb] (See further discussion below under *Adipose Tissue Thickness and Skin Melanin*.)

Arterial-Capillary-Venous Relative Contributions

Although it is recognized that the portion of the NIRS signals arising from microvascular [Hb] represents some weighted average of arterial, capillary, and venous (a, c, v) heme O_2 saturations (33, 34, 101), two questions remain currently unresolved. *1*) In either cerebral or skeletal muscle tissue, what is the relative distribution of heme units among these vascular beds (Fig. 1)? *2*) Does this distribution remain constant with interventions such as exercise, ischemia/reperfusion, changes in blood volume, and arterial P_{CO_2} and P_{O_2} (101)? Using a prototype frequency domain spectrometer, Watzman et al. (144) found in pediatric brains that the arterial and venous contribution to cerebral oxygenation was 16 ± 21% and 84 ± 21%, respectively, and was robust within each subject during normocapnic, hyperoxic, and hypoxic air breathing, but showed great intersubject variability, ranging from 40:60% to 0:100% arterial:venous contribution across subjects. Lai et al. (93), in an elegant modeling paper, assumed the relative (a, c, v) distribution in skeletal muscle to be 10:15:75% at rest, but without citation as to the source of this distribution. With exercise, they assumed the distribution to change slightly to 10:30:60%, with any change in muscle vascular volume occurring in the capillaries. Again, unfortunately, no citation was provided to support this conclusion. In contrast to this assumed distribution, Poole et al. (119) report that in the rat diaphragm, ~84% of the vascular volume is in the capillary network, with the remainder split between the arterioles and venules, based on morphometric analysis. This distribution of Hct within the a:c:v microvascular compartments is important to the extent that each compartment has a unique P_{O_2} and O_2 content. While this can be measured at the ends of the network (i.e., arterial and venous P_{O_2}) (144), there is little to no information regarding distribution of P_{O_2} (and thus oxy- and deoxy[Hb] within the network in humans, specifically $P_{cap}O_2$ versus Pa_{O_2} and Pv_{O_2} [see (34) for further discussion].

Adipose Tissue Thickness and Skin Melanin

Independent of the NIRS methodology used, factors that universally affect the signal strength are the concentration of melanin in the skin and the thickness of the tissues over the muscle(s) of interest, i.e., the adipose tissue thickness (ATT).

Melanin content in the skin is directly related to a reduction of StO_2 signal, with potential complete loss of signal during sustained isometric contractions (143). While the influence of skin melanin concentration on absorption and scattering of NIR light has been characterized (148), currently there is no generally available method to correct NIRS signals for this potential loss of signal strength.

Increasing ATT will reduce the relative contribution of the underlying skeletal muscle to the NIRS signals, resulting in greater NIR signal strength due to reduced absorption by muscle chromophores. This will appear as an overall decrease in concentration of heme chromophores in the tissue (14, 17, 139). This becomes important because the depth of the mean path length of photons is typically estimated as one-half the source-detector difference (32, 76). In addition to reducing the relative contribution of the underlying skeletal muscle to the overall NIRS response, there is indirect suggestion that during reactive hyperemia, thicker ATT may independently contribute to (contaminate?) the NIRS signals with values reflective of adipose tissue (e.g., lower metabolic rate and reduced heme concentrations) (102). If $StO_{2\%}$ is the primary NIRS outcome variable, correction for ATT may not be necessary, as both the numerator and denominator will be affected to a similar degree. However, if a system is used that provides absolute concentrations of heme (such as FD or TD systems), developing a correction factor for ATT would quantify more accurately the oxygenation characteristics of the underlying muscle(s), independent of ATT, permitting comparison across subjects with differing ATT.

When studies do correct for ATT, it is typically accomplished using linear regression of the NIRS variable of interest against either actual ATT values (14, 17, 89) or a log transformation of ATT (132, 139) or an exponential model (27) across subjects, sometimes across multiple muscle sites, then correcting individual responses based on the regression char-

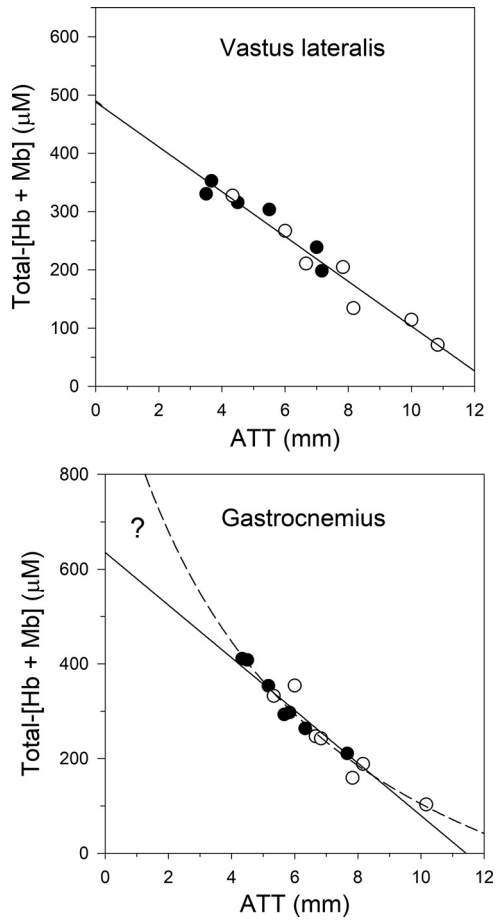

Fig. 5. Relationship between total[Hb+Mb] and adipose tissue thickness (ATT) for the vastus lateralis and gastrocnemius in 14 subjects at rest (28). ●, Men; ○, Women. Note clearly linear relationship for the vastus lateralis (r^2 = 0.954, *y*-intercept = 488, SEE = 18 μM), while the relationship for the gastrocnemius is slightly better described by a curvilinear function (linear r^2 = 0.925, *y*-intercept = 635, SEE = 30 μM; exponential r^2 = 0.947, *y*-intercept = 1,047, SEE = 83 μM). Consequence of these uncertainties (appropriate function to describe relationship and SEE for the *y*-intercept for any function) reduces the confidence in the actual group mean value for [Hb+Mb] at zero ATT. Hb, hemoglobin; Mb, myoglobin.

Downloaded from journals.physiology.org/journal/jappl (065.021.193.086) on March 4, 2022.

acteristics (slope and intercept) of the group (14, 17, 27, 87). Depending on the study, the outcome variable(s) corrected for (i.e., correlated with) ATT have included estimates of resting muscle $\dot{V}O_2$ (126, 139), the slope of deoxy[Hb+Mb] during cuff ischemia (27, 89), resting measures of total[Hb+Mb] (17, 28, 71) (Fig. 5), and dynamic changes in oxy- and deoxy-[Hb+Mb] (14). Several assumptions are fundamental to this approach, which are discussed in detail in (28).

In view of these assumptions, the sensitivity of the NIRS signals to ATT raises potentially serious concerns regarding the quality and accuracy of insight that can be gleaned from NIRS responses in subjects with appreciable ATT. Thus, specific recommendations are as follows.

Specific recommendations. For all studies:

1. ATT should be measured in every subject or patient if possible to ensure that the depth of light penetration, as estimated by one half the source-detector separation, sufficiently interrogates the underlying muscle(s) of interest as to provide meaningful information about muscle blood flow/metabolism interactions.
2. To ensure *#1*, if possible, without compromising subject characteristics, recruit subjects with lower ATT values, possibly no greater than 1/4 the longest source-detector center to center separation.

For studies incorporating FD or TD systems where absolute NIRS values are measured:

3. When making intersubject comparisons, correct data to a common value (*y*-intercept of the ATT relationship) to facilitate intersubject comparisons (17).
4. Thought should also be given as to the variable or parameter to be corrected by ATT. Intersubject variability of a response variable (e.g., slope of change during cuff ischemia, or upon cuff release, or a peak value during exercise) likely will include subject differences not attributable to ATT alone. A recommendation is to correct absolute signal strength (i.e., total[Hb+Mb] or equivalence), obtained at rest, to ATT. (See also discussion of a physiological or ischemic calibration below).

Cutaneous Blood Volume/Flow

In addition to ATT, the other potentially confounding anatomical factor affecting NIRS signals and interpretation is the potential contribution of skin blood volume/flow to the signals. By using CW systems, both local and/or whole body heating increased tissue oxygenation (as $\Delta[HbO_2 + MbO_2]$) (35) or StO_2 (21) and total[Hb+Mb] (105), while intradermal injection of epinephrine (21) and lower body negative pressure (LBNP) (48) reduced both cutaneous blood flux and StO_2 in proportion. SRS systems, however, appear to provide StO_2 and blood volume responses that are relatively insensitive to heating-induced changes in cutaneous circulation (105). It should be remembered that StO_2 is the ratio oxy[Hb+Mb]/total[Hb+Mb]. Thus, it is likely that the increase in StO_2 seen with heating reflects the increase in cutaneous oxy[Hb+Mb] with little to no effect on deoxy[Hb+Mb] (67). This was demonstrated by Koga et al. (90) using a TRS system. Assuming constant μ_s' to mimic CW instruments, oxy[Hb+Mb] increased significantly more compared with the equivalent TRS values, while the increase in deoxy[Hb+Mb] was similar between CW and TRS calculations. The oxy[Hb+Mb] signal arises mainly from longer wavelengths (>800 nm) of near-infrared light (147), which penetrate deeper into tissue (133). However, since cutaneous tissue extracts little oxygen, oxy[Hb+Mb] in cutaneous blood will be high. Thus the oxy[Hb+Mb] signal may be largely influenced by skin blood volume/flow (122).

Heterogeneity of Tissue Responses

Most original commercial NIRS systems examine one discrete volume of tissue. The assumption, therefore, was/is that the muscle(s) of interest were homogeneous, so that measurements made at one site would be reflective of any other site on the muscle/limb. In fact, several studies have demonstrated the fallacy of this assumption in muscles of the leg. For example, differences have been observed for the proximal versus distal medial (107) or lateral gastrocnemius (146), vastus lateralis versus rectus femoris (88, 89), and superficial versus deeper vastus tissue (27, 116) (see also discussion of ATT above). This heterogeneity of quadriceps oxygenation is elegantly reinforced by the latest advance in 3D imaging of muscle tissue, diffuse optical tomography (DOT) (79) (see section below for further discussion). Interpretation of the variability in tissue oxygenation at different sites is aided by simultaneous measurement of muscle activation using surface EMG (27). In addition to variability due to site heterogeneity, few if any of the studies examined or reported reproducibility, either as trial-to-trial or day-to-day. Extreme caution is thus urged regarding using a single site to predict whole muscle or whole limb responses, especially for large muscles like those of the thigh (e.g., vastus lateralis, rectus femoris). Furthermore, potential heterogeneity should be discussed as a limitation when a single probe is used on large muscles.

Validation

While development of new spectrometers includes comparing their output against phantoms of known composition and scattering characteristics, phantoms do not typically reflect the spatial heterogeneity of biological tissues (9). Ideally, physiological validation of the NIRS signals requires concomitant, quantitative knowledge as to the source of the signal(s). As discussed above, given the relative uncertainty of that, various validation approaches have been attempted. The most common (practical) approach has been to compare NIRS-derived muscle StO_2 or deoxy[heme] values to venous O_2 content draining the muscle(s) of interest, which has yielded mixed results. The reader is directed to two excellent discussions of the limitations of this approach (8, 68). In contrast, in possibly the definitive approach, Jue and associates (8, 136) compared the NIRS-derived deoxy[Hb+Mb] signal to MRS-derived deoxy[Mb] and deoxy[Hb] independently in the finger superficial flexor muscles. They found that during both exercise and cuff ischemia/reperfusion, the NIRS deoxy signal corresponded dynamically to the deoxy[Mb], but not the deoxy[Hb], signal, confirming that intramyocyte [Mb] contributes significantly to the NIRS signal.

Calibration

As noted above, both time domain and frequency domain spectrometers provide actual concentrations of the heme chromophores in the field of view. With these devices, instrument warmup and calibration following the manufacturer's recom-

Downloaded from journals.physiology.org/journal/jappl (065.021.193.086) on March 4, 2022.

mendations should be adequate. In contrast, because continuous-wave spectrometers only provide relative (changes in) signal intensity, or provide StO_2 in percent, two different strategies have primarily been employed to provide some additional quantification. One is to normalize the NIRS data to a physiological scale (called a physiological or ischemic calibration). However, variability in the technique limits the ability to extrapolate results from one study to another. Typical scaling procedures usually define 0% as the minimum value seen during arterial cuff ischemia. However, the peak value for the scale (100%) has been variously defined as the baseline value before any intervention (25, 48), peak value with local heating (35), or the peak value after cuff release (100%) (7, 16, 26, 126, 132). The last method shows excellent within-subject reproducibility for the physiological range (ICC = 0.96) and appears to remove the influence of ATT (126). However, there are several limitations to the physiological or ischemic calibration method. The procedure is not needed if the instrument output is $StO_{2\%}$, which is based on absolute (changes in) tissue [heme] saturation. In contrast, the physiological or ischemic scale is a relative scale, and as such does not quantitatively correspond to the true range of 0% to 100% StO_2, as 0% StO_2 is less than and 100% StO_2 greater than the 0% and 100% of the physiological or ischemic scale. Thus authors and readers are strongly cautioned to clarify whether the unit of data as percent is determined from the ischemic scale or from a measure of the absolute (changes in) [heme]. The approach may not be feasible in clinical or athletic studies outside a research laboratory. In addition, depending on the size and position of the occlusion cuff, the procedure can be painful. Another method, especially incorporated in the spatially resolved CW spectrometers, is to use a constant DPF in the software (37, 126, 140). As discussed above, although using a constant DPF appears to produce more semiquantitative values, the results still may not resemble the "true" responses in a given subject determined by continuous measurement of the reduced scattering coefficient (51, 53) and will still be vulnerable to confounding factors such as the ATT (126). Finally, it should be noted that CW SRS oximeters do not require calibration nor the use of DPF for StO_2% measurements.

Specific recommendations.

1. For FD and TD oximeters, warm up and calibration should be performed at least daily, but ideally before each subject/experiment depending on stability of the instrument, and the relevant values recorded. Day-to-day reproducibility should be reported. For CW oximeters where the primary/only output of interest is $StO_{2\%}$, no warm up or calibration is necessary.
2. If a physiological or ischemic calibration is desired or deemed necessary, there are several considerations which must be addressed and standardized. These include:
   a. Position of the subject—it is recommended that the entire limb being cuffed be placed horizontal so as to minimize movement of red blood cells out of, or into, the field of view.
   b. Size of the cuff—it is recommended to use as wide a cuff as feasible and effective, as this will distribute the compressive force over a larger volume of tissue, reducing the possibility of pain and/or tissue damage.
   c. Position of the cuff—the cuff should be placed as proximal on the limb as possible while still producing the desired occlusion.
   d. Inflation pressure—sufficient pressure should be applied to produce complete arterial occlusion. In the upper arm this is typically ~50 mmHg above systolic blood pressure. In the leg the effective application of the pressure is more difficult, due in part to the greater tissue volume surrounding the femoral artery. We have observed that 250–300 mmHg is necessary to produce full occlusion. This can be assessed by palpation or use of Doppler sonography of the ankle artery. Additional tricks we use include placing a rolled up towel in the region of the inguinal groove under the cuff and, when feasible, placing a weight-lifting belt over the blood pressure cuff to prevent outward expansion of the bladder and cuff.
   e. Duration of the occlusion—this typically is ~5 min and reflects a compromise between the NIRS signals reaching a plateau and discomfort to the subject. It should be recognized that if a true zero (0) plateau is desired, the occlusion duration may need to be longer or exercise added during the cuff occlusion.
   f. Speed of inflation/deflation—full inflation and deflation should be accomplished as rapidly as possible, ideally within 1–2 s. Slower times run the risk of partial perfusion occurring before complete occlusion or release.
   g. Duration of recovery—this depends in part on the research or clinical question being addressed. At a minimum, data collection should continue until the peak/minimum changes that took place with cuff release begin to subside (~2–3 min). Furthermore, if repeated cuff/release protocols are used (as with VOTs), recovery before the next trial should extend until the relevant NIRS signals (and other physiological measures as appropriate) have returned to the pre-cuff baseline.

APPLICATIONS OF NIRS

Following are several common applications of NIRS technology. At the end of some descriptions are specific recommendations to improve reproducibility and confidence in the findings. These specific recommendations are in addition to the general recommendations found at the end of this article, which are generically appropriate for all studies incorporating NIRS.

Blood Flow

It should be noted that NIRS signals per se do not measure blood flow directly. The most common method to obtain an estimate of blood flow uses a plesthysmographic approach with venous occlusion (typically 40–80 mmHg cuff) while determining the initial rate of increase in the total NIRS signal (30, 31), analogous to the initial increase in forearm circumference/volume with strain gauge plesthysmography (37). The procedure involves rapid inflation of a cuff around the limb of interest to 60–80 mmHg and tracking the rate of rise in total[Hb+Mb]. The progressive increase in tissue and venous vascular back pressure results in a curvilinear response, such that only the first 1–2 cardiac cycles of data should be used (30,

Downloaded from journals.physiology.org/journal/jappl (065.021.193.086) on March 4, 2022.

137). Intrasubject correlation coefficients comparing NIRS output to strain gauge blood flows range from 0.853 to 0.981 with associated standard errors of the estimate ranging from 0.234 to 0.986 (75), while between day reproducibility of resting blood flow shows a CV ranging from 15% (97) to 20–30% to 38–42% (132, 141). Excellent examples of the reporting of trial to trial and day-to-day reproducibility using SRS systems include the studies of Southern et al. (132) and Lucero et al. (97). Cuffing the wrist above systolic pressure during the venous occlusion significantly reduced the rate of increase in oxy-, deoxy-, and total[Hb+Mb], leading to the suggestion not to cuff the wrist (31). However, no validation regarding this recommendation was provided, except that it led to changes in the responses.

The assumptions of the plesthysmographic approach are that *1*) dynamic changes in the total [Hb+Mb] signal reflect changes in [Hb], while tissue [Mb] remains constant (34), *2*) changes in [Hb] reflect changes in blood flow (i.e., microvascular hematocrit is constant), and *3*) that scattering (as μ_s' or DPF) remains constant over the measurement period. The first assumption is reasonable, since tissue [Mb] likely will not change with acute interventions. Regarding the second assumption, during dynamic changes in muscle perfusion following the onset (85) and in recovery from muscle contractions (56) there is a transient dissociation between capillary flow and hematocrit. It is currently unclear if any dissociation between microvascular flow and [Hb]/Hct occurs during or immediately following venous or arterial cuff occlusion, cuff release, etc., and if so, to what extent this would alter the assumption that d[Hb]/d(t) reflects flow. Finally, changes in scattering and/or DPF have been reported (51) and discussed above.

The time course, or kinetics, of deoxy[Hb+Mb] following exercise onset have also been used to estimate capillary or microvascular blood flow kinetics, when limb or pulmonary $\dot{V}O_2$ has been simultaneously measured, by rearrangement of the Fick equation

$$\dot{Q}_{cap} = \frac{V_{O_2}}{(a - v)O_2} \alpha \frac{V_{O_2}}{HHb}$$

where the $(a - v)O_2$ difference is estimated by the deoxy[Hb+Mb] (52, 74). While the resulting estimation of $\dot{Q}_{cap}$ has proved insightful to circulatory control at the microvascular level, the technique has not universally produced appropriate responses. Murias et al. (112) showed that when baseline blood flow was elevated with prior exercise, the calculation of $\dot{Q}_{cap}$ produced nonexponential responses. In contrast, a normalized version of the reciprocal, as deoxy[Hb+Mb]/$\dot{V}O_2$, produced a response in which the magnitude of any overshoot of the ratio was associated with the time constant τ for $\dot{V}O_2$ kinetics [i.e., the greater the overshoot, the slower (longer τ) the $\dot{V}O_2$ kinetics] and transient $\dot{Q}O_2$ /$\dot{V}O_2$ mismatching (111).

Specific recommendations.

1. Cuff inflation to the target 60–80 mmHg should be rapid (1–2 s).
2. Calculate the slope of increase in total[Hb+Mb] using only the first 1–2 cardiac cycles.

Tissue Oxygen Uptake

Tissue oxygen uptake ($m\dot{V}O_2$) has been estimated by NIRS using the basic assumption that, during cuff occlusion, the rate of disappearance of oxy[Hb+Mb] and/or the rate of appearance of deoxy[Hb+Mb] reflect(s) the rate of oxygen utilization by the underlying muscle/tissue ($m\dot{V}O_2$). This technique has been used to estimate $m\dot{V}O_2$ in the forearm (75), calf (146), and vastus lateralis (97). Early work combined the measurement of changes in total [Hb+Mb] during venous occlusion (VO) to estimate limb blood flow with measurement of changes in deoxy [Hb+Mb] to estimate $m\dot{V}O_2$ (23, 37, 75, 141). More recently, arterial occlusion (AO), considered more accurate (140), has been used to produce a stop-flow, ischemic condition. With AO, $m\dot{V}O_2$ has been estimated from the rate of change in oxy[Hb+Mb] (23, 37, 75, 140, 141), tissue percent saturation (16), or the difference in slopes between oxy[Hb+Mb] versus deoxy[Hb+Mb] (Hb_{diff} = oxy[Hb+Mb] – deoxy[Hb+Mb]) (36, 51, 97, 140, 141). With these techniques, between-day CV for resting muscle $\dot{V}O_2$ range from 12 to 22% (132) to 18% (140) to 50% (97). CV across a range of work intensities is fairly constant at 13–24% (97). A further correction of the NIRS signals can be applied to account for any shifts in "blood volume" during the cuff period, i.e., movement of RBCs from high pressure NIRS invisible (arterial vessels > 1 mm diameter) segments to lower pressure, NIRS visible (capillaries and small venules) segments (101, 126). In addition, when Hb_{diff} is used and quantitative $\dot{V}O_2$ values are desired, the resulting calculation(s) should be divided by 2 to correct for the fact that Hb_{diff} represents the sum of two slopes (51, 97, 140).

$m\dot{V}O_2$ has also been estimated during free flowing exercise, as the product of an independent measure of blood flow (typically with Doppler ultrasound) and the deoxy[Hb+Mb] (20, 74). The assumption here is that the conduit artery blood flow reflects the microvascular flow associated with the deoxy[Hb+Mb] signal where gas exchange takes place. However, recent studies using either indocyanine green (72) or diffuse correlation spectroscopy (DCS) (73) have shown a plateauing of microvascular blood flow at higher aerobic work rates, with the latter study directly showing a dissociation of microvascular from brachial artery blood flow at high work rates, suggesting this relationship is more complicated than originally believed.

Specific recommendations.

1. Calculate the slopes of change in deoxy[Hb+Mb] and oxy[Hb+Mb] only during the initial linear portion of the responses (typically ~1 min for resting measurements, but likely much shorter (e.g., 10–15 s) when metabolic rate is higher as with exercise).
2. Use $Hb_{diff}/2$ to estimate the rate of O_2 extraction.
3. Correct for changes in blood volume signal, especially if using a CW instrument.

Oxidative Capacity (as $\tau\dot{V}O_2$)

Ryan et al. (126) developed a protocol, reviewed in (145), to estimate mitochondrial, or oxidative "capacity," by extracting an apparent time constant for $m\dot{V}O_2$ in recovery following a single intense contraction, produced either voluntarily or by electrical stimulation. The time course for the recovery of $m\dot{V}O_2$ is determined from a series of brief supra-arterial cuff

Downloaded from journals.physiology.org/journal/jappl (065.021.193.086) on March 4, 2022.

occlusions. The resulting time constant has been validated against ^{31}P-MRS determination of PCr recovery kinetics (128) and in permeabilized muscle fiber bundles (125). The technique has also been applied to evaluate patient populations (124, 127, 131). Coefficient of variation is good (~10%), but the intraclass correlation coefficients range from 0.26 to 0.93 (1, 126, 132). Adami and Rossiter (2) recently discussed the procedure and necessary precautions.

Specific recommendations.

1. Contraction effort should be intense but not close to maximal, so as to adequately stimulate oxidative phosphorylation in the muscle, and last for 10–15 s.
2. Determine the contraction effort and duration such that StO_2 remains above 50% of this functional range.
3. Correct for changes in hemoglobin volume.
4. Ensure that the occlusions do indeed occlude the arterial inflow each time.
5. ATT should be low enough to ensure that the specific NIRS probe being used adequately interrogates the underlying muscle(s).
6. Average 2–3 trials for each subject to minimize variability and enhance signal:noise.

Postocclusive Reactive Hyperemia/Vascular Occlusion Test

One of the most common clinical applications of NIRS is the PORH test, or VOT, which seeks to assess endothelial (vascular) function or reactivity. The test consists of arterial occlusion for a period of time, typically 5 min, followed by cuff release. NIRS signals are tracked at baseline, throughout the occlusion period, and following cuff release for 3–5 min (Fig. 6). Originally, vascular responses were monitored by ultrasound, with the peak vasodilation of the artery (flow mediated dilation FMD) determined 50–60 s after cuff release (24). The vast majority of studies have utilized muscles of the upper limb [forearm or the thenar eminence (117)] or lower leg (104)). Two phases of the experiment are typically analyzed: the initial change in NIRS signals during the first 1–2 min of occlusion for determination of $m\dot{V}O_2$, usually performed on forearm muscle (Slope 1, discussed above under *Tissue Oxygen Uptake*), and the end-cuff and early rapid dynamic changes in NIRS signals following cuff release (Fig. 6, *slope 2*). The early rapid changes have been analyzed in a variety of ways. Bopp and associates (15) used sigmoid (Gompertz and logistic) functions to describe the early phase of change in oxy- and deoxy[Hb+Mb] and a double exponential model for the changes in the total[Hb+Mb] signal. While three trials were performed in both studies, no measures of variability or reproducibility were provided. The most common description of reactive hyperemic changes has been a linear description of the initial rise in the StO_2 signal upon cuff release, referred to as the reperfusion slope or rate (117) or slope 2 (103) (Fig. 6). In healthy subjects this slope correlates with percent flow mediated dilation (103), duration of cuff occlusion, and training status (104), and is altered

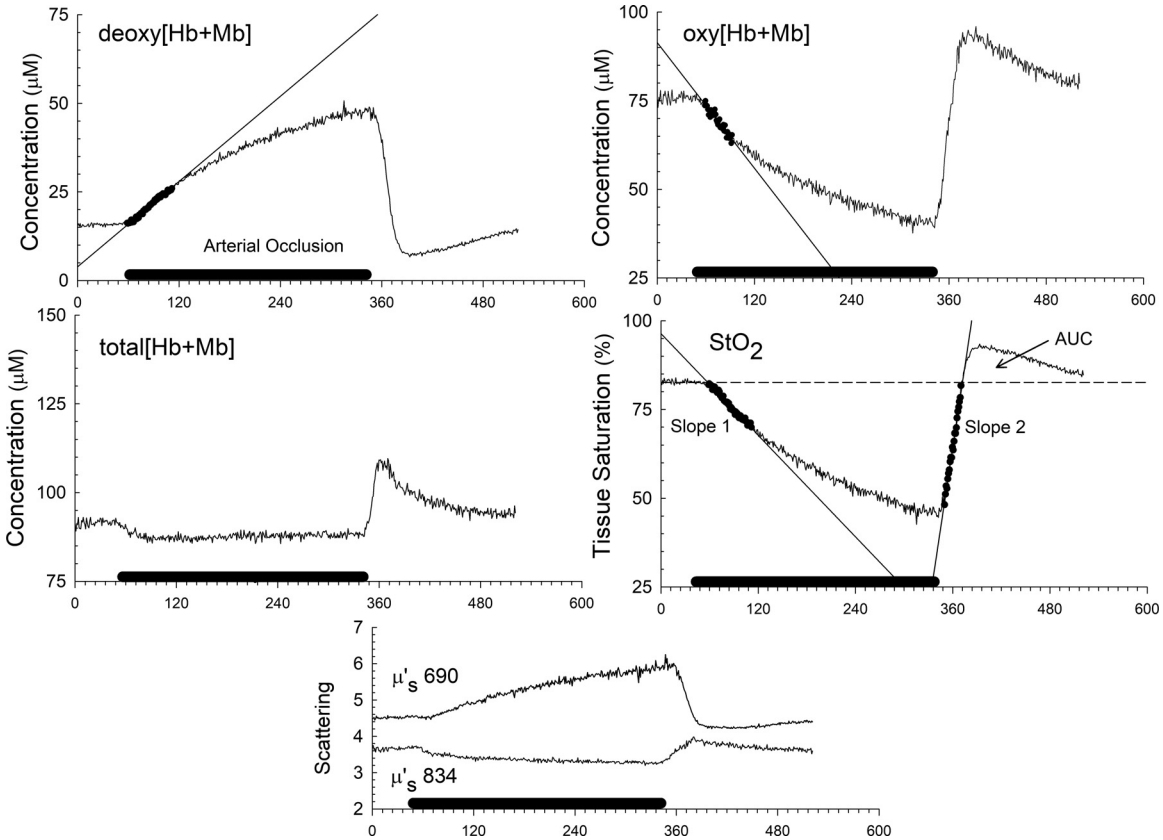

Fig. 6. NIRS signal responses and reduced scattering coefficients (μ_s') during a postocclusive reactive hyperemia (PORH)/vascular occlusion test (VOT) test in a representative subject. Linear slope lines for deoxy[Hb+Mb] and oxy[Hb+Mb] during the first minute (*slope 1*) can be used to calculate resting muscle metabolism ($m\dot{V}O_2$) (see text above). *Slope 2* of StO_2, also referred to as the reperfusion slope, is used to assess the relative speed of re-oxygenation following cuff release. AUC, area above baseline StO_2 following cuff release. Note changes in the reduced scattering coefficient (μ_s') for 690 nm and 834 nm. Hb, hemoglobin; Mb, myoglobin.

Downloaded from journals.physiology.org/journal/jappl (065.021.193.086) on March 4, 2022.

(slowed) in healthy subjects at altitude (100) and in patients with septic shock (29, 96, 117), pulmonary arterial hypertension (42), and circulatory failure (96). In addition, the area above the baseline following cuff release (AUC in Fig. 6) has been shown to be predictive of 90-day survival rate upon admission to the ICU (43). While much of the clinical literature has focused on *slope 2* determined in the thenar eminence, forearm musculature may be more sensitive to changes in the peripheral circulation than the thenar eminence (10). This last point should be further investigated.

Specific recommendations.

1. Arterial occlusion (typically 50 mmHg over systolic for arm, 100 mmHg over systolic for leg experiments) should be applied for 3–5 min. If possible, effectiveness of the occlusion should be confirmed by the absence of downstream blood flow or pulses. Application of pressure, and its removal, should be rapid (e.g., within 1–2 s).
2. Multiple trials (2-3) should be performed with sufficient time between repeated bouts (~10–15 min) provided so that the relevant signals return to baseline. This should be confirmed and documentation provided. If multiple trials are performed, the possibility of alterations in large vessel reactivity should be ruled out (e.g., an order effect to the responses).
3. The reperfusion slope after cuff release (*slope 2* in Fig. 6) can be described either as a slope or a half-time. If the slope is calculated, only the initial linear rise of StO_2 (e.g., from lowest value at cuff release up to approximately the original baseline value) should be used.
4. For any fitting function used on any response, the coefficient of determination for the overall fit, and the SEE for each parameter should be provided.

EXERCISE

One of the most frequent applications of NIRS has been to track tissue/muscle oxygenation during exercise. Within this broad topic, the two most common examples are incremental exercise to task failure and abrupt step or square-wave increases and decreases in work rate.

Incremental Exercise

NIRS signals have been used during incremental ramp-type exercise to describe tissue oxygenation responses throughout the range of exercise intensities. Celie et al. (25) described the changes in deoxy[Hb+Mb] and StO_2 (SmO_2) during discontinuous incremental handgrip exercise. The patterns of both signals increased approximately linearly from 20% to 50% MVC, with a slight upward trend at the highest work rate (~70% MVC). Day-to-day reproducibility was very good (ICC at peak exercise was 0.87 for deoxy[Hb+Mb] and 0.77 for StO_2). The pattern of change in the quadriceps during cycling, especially as the limit of exercise tolerance is approached, has been described most often using either a sigmoid function (13, 54, 83, 94, 106, 120), or a breakpoint model (12, 83). In turn, the break point for deoxy[Hb+Mb] has been shown to correlate with the Respiratory Compensation Point in some (61, 83) but not all (18, 19) studies. Furthermore, the break point for deoxy[Hb+Mb] has shown significant correlation with the maximum lactate steady state and critical power (83). Earlier work also reported a significant relationship between changes in the pattern of absorption using a CW instrument and the ventilatory or lactate threshold (11, 69) and positive correlations ($r = 0.89$) between an inflection point of the oxygenation index and both mean arterial pressure and vascular resistance in the distal, but not proximal, regions of the calf (108). More recently, Wang et al. (142) found strong correlations ($r = 0.95–0.99$) between breakpoints in the ΔDeoxy[Hb+Mb] and tissue oxygenation index (TOI) responses and the estimated lactate threshold.

Unfortunately, there is a paucity of reporting of measures of parameter confidence intervals, within day and day-to-day reproducibility for the parameters of interest, including break points for NIRS, Respiratory Compensation Point, and the slope of a sigmoid fit. Confidence intervals for the intersection of two lines (break points) should be calculated using the following references (5, 82).

Square Wave Transitions (Kinetics)

NIRS has also been used to examine the relative matching of oxygen delivery (as $\dot{Q}O_2$) with tissue oxygen utilization ($\dot{V}O_2$) following the sudden increase or decrease in work rate, during cycle ergometry (39, 57, 67), knee extension exercise (45, 74), and plantar flexion exercise (95). The kinetics of increase of deoxy[Hb+Mb] following exercise onset have been studied the most, modeled as an exponential process, with a time constant and delay (39, 67, 88), or as the ratio of normalized deoxy[Hb+Mb]/$\dot{V}O_2$ (111, 112, 120). (It should be noted that the normalized ratio is generated from a global pulmonary $\dot{V}O_2$ and a specific site for deoxy[Hb+Mb], which given the discussion above regarding heterogeneity, will not reflect the diversity of actual ratios within the quadriceps muscles.) An overshoot in the normalized ratio deoxy[Hb+Mb]/$\dot{V}O_2$ has been interpreted as indicating an impairment in O_2 delivery relative to O_2 utilization following exercise onset, being greater after bedrest (120) and reduced following endurance training (109). The kinetics of deoxy[Hb+Mb] are inversely related to $\dot{V}O_2$ kinetics (i.e., faster deoxy[Hb+Mb] kinetics are associated with slower $\dot{V}O_2$ kinetics) (Fig. 7), both acutely (67) and following prior warmup exercise (38, 110) and endurance training (109), and are positively correlated with $\dot{V}O_2$ peak in patients with metabolic myopathies (66). In virtually none of these studies was either the SEE of the kinetic parameters provided for each curve fit in each subject, or any measure of day-to-day reproducibility.

Specific recommendations.

1. Parameter estimate confidence (as SEE) and day-to-day reproducibility (ICC) of the key parameters need to be assessed and reported.
2. When applying a break point model to incremental exercise data, the actual break point is determined as the intersection of two straight lines and should be visually compared with the raw data to ensure that the break point lies within the general trend of the data (i.e., there truly is a point of intersection or break point in the raw data, as opposed to a smooth curve of transition).
3. A plot of residuals should be provided for each subject and curve fit to verify overall goodness of fit.
4. To describe the initial response of deoxy[Hb+Mb] to a square wave increase in work rate, it is suggested to use a monoexponential function with time delay for the data

Downloaded from journals.physiology.org/journal/jappl (065.021.193.086) on March 4, 2022.

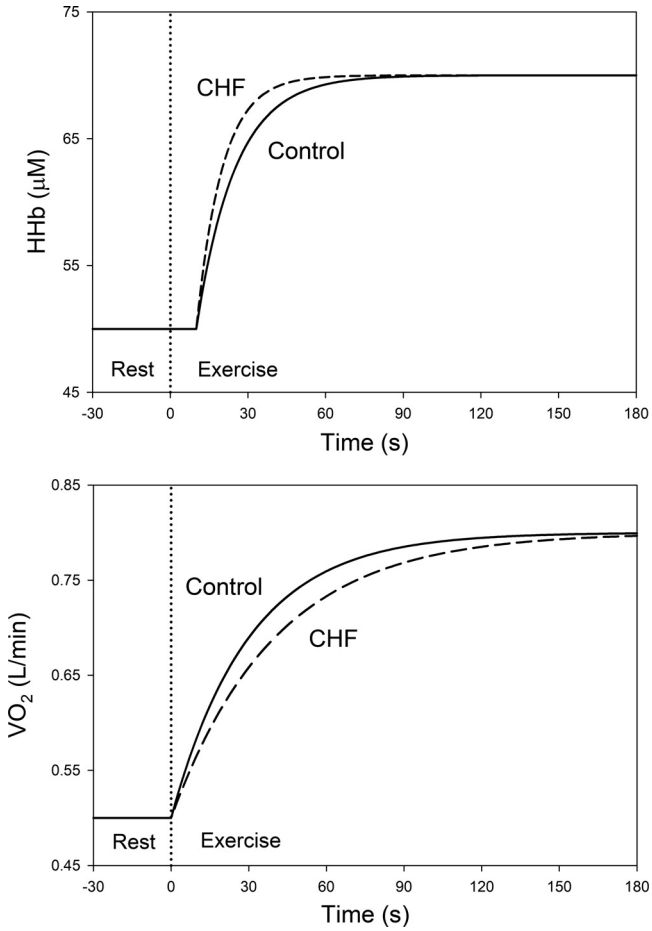

Fig. 7. Schematic showing the inverse relationship observed between $\dot{V}O_2$ kinetics and the kinetics of deoxy[Hb+Mb] (HHb). Start of exercise shown by dotted line. Slower $\dot{V}O_2$ kinetics [e.g., patient with cardiac heart failure (CHF)] are associated with faster deoxy[Hb+Mb] kinetics (dashed line for both responses), indicative of a relatively sluggish adjustment of blood flow relative to muscle $\dot{V}O_2$. Note that the differences in kinetics of both responses are resolved by the time steady state is reached in this example. Hb, hemoglobin; Mb, myoglobin.

from ~30 s before exercise onset to the peak value (typically 90–120 s into exercise).

NEWEST TECHNOLOGIES

Recent advances in NIRS show great promise in providing exciting new insights into muscle metabolism and microvascular blood flow; these include diffuse correlation spectroscopy (DCS) and diffuse optical tomography (DOT). DCS uses coherent NIR light to penetrate deep tissues and measure speckle fluctuations of the diffuse light caused primarily by the motion of red blood cells to provide a microvascular blood flow index. The correlation equations and algorithms used for DCS have been described in detail by Durduran and Yodh (47). An example of the application of DCS to exercise responses is the work by Hammer et al. (73) using the MetaOx system (ISS). Diffuse optical tomography uses sophisticated multiple source-detector NIRS data collection and algorithms to generate a 3D image of tissue oxygenation (78). As with DCS, to date there has been limited application of DOT to exercising muscle (79). Finally, the development of a low-cost, small-size, low-power TRS system for clinical use (tNIRS-1, Hamamatsu, Japan) (65) provides an opportunity to bring truly quantitative NIRS to the clinical bedside. Other applications of NIRS to sports and clinical situations are described in the excellent review by Grassi and Quaresima (68).

Is There an "Ideal" NIRS Oximeter?

A single "ideal" NIRS system may not exist, due to the different requirements for different applications. Nonetheless, a single system that would meet many of the needs detailed above might be based around technology that *1*) provides dynamic measurement of scattering and/or actual DPF values, with appropriate incorporation into calculation of actual chromophore concentrations (i.e., either FD or TD based). *2*) Determination of heterogeneity across the muscle site(s) of interest would be advantageous, especially for the larger muscles of the legs. *3*) Portability would extend tremendously the application into both athletic and clinical settings. *4*) Inclusion of correction for ATT would facilitate comparisons of actual concentrations across subjects, although use of $StO_{2\%}$ may obviate this feature. *5*) The ability to detect the relative oxygenation status of tissue cytochrome aa_3 would provide currently unobtainable information regarding the final chromophore in the O_2 diffusion pathway. *6*) Finally, probes that would permit penetration depths beyond the current commercially available ones would facilitate examination of subjects with greater ATT (obese and/or patients) as well as provide the opportunity to examine heterogeneity by depth of muscle recruitment and O_2 delivery to utilization matching in the muscles of the thigh (Table 2).

SUMMARY/GENERAL RECOMMENDATIONS

Several recent reviews have included recommendations to improve the quality and reproducibility of NIRS data collection and interpretation (2, 50, 118). The following is a summary of these recommendations expanded to include the relevant points raised in this CORP. These recommendations are generically

Table 2.

What we now know because of NIRS
• Contribution of myoglobin to the NIRS signal is significant.
• Large muscles often demonstrate spatial and depth heterogeneity.
• Microvascular hematocrit increases with exercise, Post Occlusive Reactive Hyperemia.
• With quantitative NIRS [time domain (TD) or frequency domain (FD)], perfusive and diffusive components of the Wagner diagram can be identified and their roles in O_2 delivery assessed.
• Muscle oxidative capacity (as $\tau\dot{V}O_2$) can be estimated noninvasively.
• Muscle $\dot{V}O_2$ during rest and exercise can be estimated.
• Survival outcomes can be predicted in severely ill patients.
What we still don't know
• Magnitude of the error in assuming Differential Path length Factor to be/remain constant across subjects and protocols.
• Circumstances wherein a physiological calibration is recommended.
• If a physiological calibration obviates the need to measure, correct for adipose tissue thickness.
• Actual values and heterogeneity of $\dot{Q}O_2$ and $\dot{V}O_2$ at the microvascular/myocyte level.
• Extent to which ignoring muscle heterogeneity in large muscles might lead to inaccurate conclusions.

NIRS, near infrared spectroscopy.

Downloaded from journals.physiology.org/journal/jappl (065.021.193.086) on March 4, 2022.

valid for all experiments and reports involving the use of NIRS.

Study Overview

Protocol. The protocol should be described in complete detail so that others can replicate it. This should include timing of all measurements.

Subjects. Complete description should be provided, including sex, age, height, weight, activity, and/or fitness levels if appropriate.

Reproducibility. The study design should include data collection to examine intrasubject reproducibility, both within day (multiple trials) and day-to-day variability (ICC).

Data Collection

Calibration. For CW systems, a physiological calibration could be used (but see discussion above) based on StO_2, consisting of 5 min ischemic cuff to produce 0% reference point, with the subsequent peak value observed after cuff release assigned 100%. For TRS or FD systems, use calibration block or other method recommended by manufacturer. Stability (before/after experiment) and day-to-day variability in calibration should be reported for all NIR spectrometers.

Probe design. The probe design should be described, including source-detector separation distances and wavelengths used.

Probe position. Probe position should be described with accurate anatomical landmarks. Orientation of probe relative to muscle length and/or fiber orientation should be described if possible. Position of probe should be marked on the skin with indelible ink if repeated applications are performed. EMG can be useful in identifying desired muscles, such as in the forearm (73).

Probe attachment to skin. Ideally, probe should be attached with medical transparent double-sided adhesive. If soft elastic bandage is used, care should be taken to use the lightest pressure necessary to eliminate probe movement while not compressing the skin/ATT. Skin locations with an abundance of dark hair should be shaved. Once positioned and attached, probe should be covered to prevent ambient light from contaminating the field of examination.

Underlying muscle geometry. If possible, ultrasound or MRI should be used to describe the length/width/depth of the interrogated muscle at the site of probe position. This is especially important when muscle geometry may be smaller than anticipated muscle volume of interrogation from probe design [source-detector distance(s)], e.g., forearm musculature.

Adipose tissue thickness. Thickness should be measured at site of probe position, either by skinfold calipers (value/2), ultrasound, or MRI.

Muscle activation. For exercise studies, muscle activation/recruitment using EMG may provide useful ancillary information. If used, the magnitude of the EMG bursts should be reported either as integrated EMG or as RMS and scaled to that seen with fresh (unexercised muscle) MVC. As with the NIRS probe, for multiple visits, the EMG electrode placement should be marked with indelible ink and described anatomically.

Data Processing/Analysis

Data processing. Given that NIRS signals from skeletal muscles have an unknown relative contribution of [Hb] and [Mb] to the signal, it is suggested that the values be reported in units of [Heme]. To accomplish this, some commercial systems (e.g., OxyplexTS, Oxymon, Portamon) require multiplying output signals by 4 to return the hemoglobin-corrected concentrations back to units of heme. In addition, in systems where μ_s' is directly measured (OxiplexTS), the window or number of data points used to estimate μ_s' should be reported.

Analyze and report all collected data. All data that are collected should be analyzed and reported, including total[Hb+Mb], StO_2, and when available, oxy- and deoxy[Hb+Mb].

Reproducibility. Intertrial and day-to-day variability of the relevant outcome variables (e.g., peak values, slopes, kinetic parameters) should be reported. Absolute reliability (intrasubject) should be assessed using limits of agreement and coefficient of variation for trial-to-trial and day-to-day variability, while relative reliability (across subjects) should be reported using intraclass correlation coefficients.

ATT. If ATT is corrected for using linear or curvilinear regression, the values and SEE for each parameter (e.g., both the slope and intercept for a linear function) should be reported (17, 28). In addition, it is recommended that total signal strength (as total[Hb+Mb]) be used for the ATT correction.

DPF. The use of a constant, universal DPF for all subjects and conditions is discouraged, as this results in only multiplying all values by the same constant number. This gives the false impression that the resulting values are correct and accurate for all subjects and conditions, and remains constant throughout a protocol. This multiplication does not change the inherent relationships between subjects or responses; thus comparisons of the raw signals (as ΔOD) will produce the same results.

Correction for blood volume changes. For protocols using CW instruments that include venous or arterial cuffing, exercise, tilt table, etc., where the total[Hb+Mb] might change, a correction for blood volume changes should be applied. The need for this correction to TRS- or FD-derived data remains to be determined.

Summary Recommendations for Field Settings (Clinical, Sports Applications)

While the above recommendations represent best practice and science, circumstances may not permit or facilitate implementation of all of the above recommendations. Given this, the following represent a realistic subset of recommendations for applied (field) setting such as might be encountered clinically or in sports settings. The reader is referred to the expanded description of each recommendation in the general recommendations above.

Study overview. Protocol, subjects, ideally reproducibility if possible.

Data collection. Calibration (if appropriate for the instrument); probe design; probe position; probe attachment to skin; adipose tissue thickness.

Data processing. All sub-topics, with the possible exception of Reproducibility and Correction for Blood Volume Changes.

DISCLOSURES

No conflicts of interest, financial or otherwise, are declared by the author.

Downloaded from journals.physiology.org/journal/jappl (065.021.193.086) on March 4, 2022.

AUTHOR CONTRIBUTIONS

T.J.B. conceived and designed research; performed experiments; analyzed data; interpreted results of experiments; prepared figures; drafted manuscript; edited and revised manuscript; approved final version of manuscript.

REFERENCES

1. **Adami A, Cao R, Porszasz J, Casaburi R, Rossiter HB.** Reproducibility of NIRS assessment of muscle oxidative capacity in smokers with and without COPD. *Respir Physiol Neurobiol* 235: 18–26, 2017. doi:10.1016/j.resp.2016.09.008.
2. **Adami A, Rossiter HB.** Principles, insights, and potential pitfalls of the noninvasive determination of muscle oxidative capacity by near-infrared spectroscopy. *J Appl Physiol (1985)* 124: 245–248, 2018. doi:10.1152/japplphysiol.00445.2017.
3. **Balaban RS, Mootha VK, Arai A.** Spectroscopic determination of cytochrome c oxidase content in tissues containing myoglobin or hemoglobin. *Anal Biochem* 237: 274–278, 1996. doi:10.1006/abio.1996.0239.
4. **Bale G, Elwell CE, Tachtsidis I.** From Jöbsis to the present day: a review of clinical near-infrared spectroscopy measurements of cerebral cytochrome-c-oxidase. *J Biomed Opt* 21: 091307, 2016. doi:10.1117/1.JBO.21.9.091307.
5. **Beaver WL, Wasserman K, Whipp BJ.** A new method for detecting anaerobic threshold by gas exchange. *J Appl Physiol (1985)* 60: 2020–2027, 1986. doi:10.1152/jappl.1986.60.6.2020.
6. **Bekedam MA, van Beek-Harmsen BJ, van Mechelen W, Boonstra A, van der Laarse WJ.** Myoglobin concentration in skeletal muscle fibers of chronic heart failure patients. *J Appl Physiol (1985)* 107: 1138–1143, 2009. doi:10.1152/japplphysiol.00149.2009.
7. **Belardinelli R, Barstow TJ, Porszasz J, Wasserman K.** Changes in skeletal muscle oxygenation during incremental exercise measured with near infrared spectroscopy. *Eur J Appl Physiol Occup Physiol* 70: 487–492, 1995. doi:10.1007/BF00634377.
8. **Bendahan D, Chatel B, Jue T.** Comparative NMR and NIRS analysis of oxygen-dependent metabolism in exercising finger flexor muscles. *Am J Physiol Regul Integr Comp Physiol* 313: R740–R753, 2017. doi:10.1152/ajpregu.00203.2017.
9. **Benni PB, MacLeod D, Ikeda K, Lin HM.** A validation method for near-infrared spectroscopy based tissue oximeters for cerebral and somatic tissue oxygen saturation measurements. *J Clin Monit Comput*, 32: 269–284, 2018. doi:10.1007/s10877-017-0015-1.
10. **Bezemer R, Karemaker JM, Klijn E, Martin D, Mitchell K, Grocott M, Heger M, Ince C.** Simultaneous multi-depth assessment of tissue oxygen saturation in thenar and forearm using near-infrared spectroscopy during a simple cardiovascular challenge. *Crit Care* 13, *Suppl* 5: S5, 2009. doi:10.1186/cc8003.
11. **Bhambhani YN, Buckley SM, Susaki T.** Detection of ventilatory threshold using near infrared spectroscopy in men and women. *Med Sci Sports Exerc* 29: 402–409, 1997. doi:10.1097/00005768-199703000-00017.
12. **Boone J, Barstow TJ, Celie B, Prieur F, Bourgois J.** The interrelationship between muscle oxygenation, muscle activation, and pulmonary oxygen uptake to incremental ramp exercise: influence of aerobic fitness. *Appl Physiol Nutr Metab* 41: 55–62, 2016. doi:10.1139/apnm-2015-0261.
13. **Boone J, Koppo K, Barstow TJ, Bouckaert J.** Pattern of deoxy[Hb+Mb] during ramp cycle exercise: influence of aerobic fitness status. *Eur J Appl Physiol* 105: 851–859, 2009. doi:10.1007/s00421-008-0969-2.
14. **Bopp CM, Townsend DK, Barstow TJ.** Characterizing near-infrared spectroscopy responses to forearm post-occlusive reactive hyperemia in healthy subjects. *Eur J Appl Physiol* 111: 2753–2761, 2011. doi:10.1007/s00421-011-1898-z.
15. **Bopp CM, Townsend DK, Warren S, Barstow TJ.** Relationship between brachial artery blood flow and total [hemoglobin+myoglobin] during post-occlusive reactive hyperemia. *Microvasc Res* 91: 37–43, 2014. doi:10.1016/j.mvr.2013.10.004.
16. **Boushel R, Pott F, Madsen P, Rådegran G, Nowak M, Quistorff B, Secher N.** Muscle metabolism from near infrared spectroscopy during rhythmic handgrip in humans. *Eur J Appl Physiol Occup Physiol* 79: 41–48, 1998. doi:10.1007/s004210050471.
17. **Bowen TS, Rossiter HB, Benson AP, Amano T, Kondo N, Kowalchuk JM, Koga S.** Slowed oxygen uptake kinetics in hypoxia correlate with the transient peak and reduced spatial distribution of absolute skeletal muscle deoxygenation. *Exp Physiol* 98: 1585–1596, 2013. doi:10.1113/expphysiol.2013.073270.
18. **Broxterman RM, Ade CJ, Barker T, Barstow TJ.** Influence of pedal cadence on the respiratory compensation point and its relation to critical power. *Respir Physiol Neurobiol* 208: 1–7, 2015. doi:10.1016/j.resp.2014.12.008.
19. **Broxterman RM, Ade CJ, Craig JC, Wilcox SL, Schlup SJ, Barstow TJ.** The relationship between critical speed and the respiratory compensation point: Coincidence or equivalence. *Eur J Sport Sci* 15: 631–639, 2015. doi:10.1080/17461391.2014.966764.
20. **Broxterman RM, Ade CJ, Wilcox SL, Schlup SJ, Craig JC, Barstow TJ.** Influence of duty cycle on the power-duration relationship: observations and potential mechanisms. *Respir Physiol Neurobiol* 192: 102–111, 2014. doi:10.1016/j.resp.2013.11.010.
21. **Buono MJ, Miller PW, Hom C, Pozos RS, Kolkhorst FW.** Skin blood flow affects in vivo near-infrared spectroscopy measurements in human skeletal muscle. *Jpn J Physiol* 55: 241–244, 2005. doi:10.2170/jjphysiol.T649.
22. **Calbet JA, Gonzalez-Alonso J, Helge JW, Søndergaard H, Munch-Andersen T, Boushel R, Saltin B.** Cardiac output and leg and arm blood flow during incremental exercise to exhaustion on the cycle ergometer. *J Appl Physiol (1985)* 103: 969–978, 2007. doi:10.1152/japplphysiol.01281.2006.
23. **Casavola C, Paunescu LA, Fantini S, Gratton E.** Blood flow and oxygen consumption with near-infrared spectroscopy and venous occlusion: spatial maps and the effect of time and pressure of inflation. *J Biomed Opt* 5: 269–276, 2000. doi:10.1117/1.429995.
24. **Celermajer DS, Sorensen KE, Gooch VM, Spiegelhalter DJ, Miller OI, Sullivan ID, Lloyd JK, Deanfield JE.** Non-invasive detection of endothelial dysfunction in children and adults at risk of atherosclerosis. *Lancet* 340: 1111–1115, 1992. doi:10.1016/0140-6736(92)93147-F.
25. **Celie B, Boone J, Van Coster R, Bourgois J.** Reliability of near infrared spectroscopy (NIRS) for measuring forearm oxygenation during incremental handgrip exercise. *Eur J Appl Physiol* 112: 2369–2374, 2012. doi:10.1007/s00421-011-2183-x.
26. **Chance B, Dait MT, Zhang C, Hamaoka T, Hagerman F.** Recovery from exercise-induced desaturation in the quadriceps muscles of elite competitive rowers. *Am J Physiol Cell Physiol* 262: C766–C775, 1992. doi:10.1152/ajpcell.1992.262.3.C766.
27. **Chin LMK, Kowalchuk JM, Barstow TJ, Kondo N, Amano T, Shiojiri T, Koga S.** The relationship between muscle deoxygenation and activation in different muscles of the quadriceps during cycle ramp exercise. *J Appl Physiol (1985)* 111: 1259–1265, 2011. doi:10.1152/japplphysiol.01216.2010.
28. **Craig JC, Broxterman RM, Wilcox SL, Chen C, Barstow TJ.** Effect of adipose tissue thickness, muscle site, and sex on near-infrared spectroscopy derived total-[hemoglobin + myoglobin]. *J Appl Physiol (1985)* 123: 1571–1578, 2017. doi:10.1152/japplphysiol.00207.2017.
29. **Creteur J, Carollo T, Soldati G, Buchele G, De Backer D, Vincent JL.** The prognostic value of muscle StO2 in septic patients. *Intensive Care Med* 33: 1549–1556, 2007. doi:10.1007/s00134-007-0739-3.
30. **Cross TJ, Sabapathy S.** The impact of venous occlusion per se on forearm muscle blood flow: implications for the near-infrared spectroscopy venous occlusion technique. *Clin Physiol Funct Imaging* 37: 293–298, 2017. doi:10.1111/cpf.12301.
31. **Cross TJ, van Beekvelt M, Constantini K, Sabapathy S.** Measurement of regional forearm muscle haemodynamics via the near-infrared spectroscopy venous occlusion technique: the impact of hand circulatory occlusion. *Physiol Meas* 35: 2563–2573, 2014. doi:10.1088/0967-3334/35/12/2563.
32. **Cui W, Kumar C, Chance B.** Experimental study of migration depth for the photons measured at sample surface. I. Time-resolved spectroscopy and imaging. *Proc Int Soc Opt Eng* 1431: 180–191, 1991. doi:10.1117/12.44189
33. **Culver JP, Durduran T, Furuya D, Cheung C, Greenberg JH, Yodh AG.** Diffuse optical tomography of cerebral blood flow, oxygenation, and metabolism in rat during focal ischemia. *J Cereb Blood Flow Metab* 23: 911–924, 2003. doi:10.1097/01.WCB.0000076703.71231.BB.
34. **Davis ML, Barstow TJ.** Estimated contribution of hemoglobin and myoglobin to near infrared spectroscopy. *Respir Physiol Neurobiol* 186: 180–187, 2013. doi:10.1016/j.resp.2013.01.012.
35. **Davis SL, Fadel PJ, Cui J, Thomas GD, Crandall CG.** Skin blood flow influences near-infrared spectroscopy-derived measurements of tissue

Downloaded from journals.physiology.org/journal/jappl (065.021.193.086) on March 4, 2022.

oxygenation during heat stress. *J Appl Physiol (1985)* 100: 221–224, 2006. doi:10.1152/japplphysiol.00867.2005.

36. **De Blasi RA, Almenrader N, Aurisicchio P, Ferrari M.** Comparison of two methods of measuring forearm oxygen consumption (VO2) by near infrared spectroscopy. *J Biomed Opt* 2: 171–175, 1997. doi:10.1117/12.269893.
37. **De Blasi RA, Ferrari M, Natali A, Conti G, Mega A, Gasparetto A.** Noninvasive measurement of forearm blood flow and oxygen consumption by near-infrared spectroscopy. *J Appl Physiol (1985)* 76: 1388–1393, 1994. doi:10.1152/jappl.1994.76.3.1388.
38. **DeLorey DS, Kowalchuk JM, Heenan AP, Dumanoir GR, Paterson DH.** Prior exercise speeds pulmonary O2 uptake kinetics by increases in both local muscle O2 availability and O2 utilization. *J Appl Physiol (1985)* 103: 771–778, 2007. doi:10.1152/japplphysiol.01061.2006.
39. **DeLorey DS, Kowalchuk JM, Paterson DH.** Relationship between pulmonary O2 uptake kinetics and muscle deoxygenation during moderate-intensity exercise. *J Appl Physiol (1985)* 95: 113–120, 2003. doi:10.1152/japplphysiol.00956.2002.
40. **Delpy DT, Cope M.** Quantification in tissue near-infrared spectroscopy. *Philos Trans R Soc Lond, B* 352: 649–659, 1997. doi:10.1098/rstb.1997.0046.
41. **Delpy DT, Cope M, van der Zee P, Arridge S, Wray S, Wyatt J.** Estimation of optical pathlength through tissue from direct time of flight measurement. *Phys Med Biol* 33: 1433–1442, 1988. doi:10.1088/0031-9155/33/12/008.
42. **Dimopoulos S, Tzanis G, Manetos C, Tasoulis A, Mpouchla A, Tseliou E, Vasileiadis I, Diakos N, Terrovitis J, Nanas S.** Peripheral muscle microcirculatory alterations in patients with pulmonary arterial hypertension: a pilot study. *Respir Care* 58: 2134–2141, 2013. doi:10.4187/respcare.02113.
43. **Donati A, Damiani E, Domizi R, Scorcella C, Carsetti A, Tondi S, Monaldi V, Adrario E, Romano R, Pelaia P, Singer M.** Near-infrared spectroscopy for assessing tissue oxygenation and microvascular reactivity in critically ill patients: a prospective observational study. *Crit Care* 20: 311, 2016. doi:10.1186/s13054-016-1500-5.
44. **Drabkin DL.** The distribution of the chromoproteins hemoglobin, myoglobin and cytochrome c in the tissues of different species and the relationship of the total content of each chromoprotein to body mass in tissues. *J Biol Chem* 182: 317–349, 1950.
45. **duManoir GR, DeLorey DS, Kowalchuk JM, Paterson DH.** Differences in exercise limb blood flow and muscle deoxygenation with age: contributions to O2 uptake kinetics. *Eur J Appl Physiol* 110: 739–751, 2010. doi:10.1007/s00421-010-1546-z.
46. **Duncan A, Meek JH, Clemence M, Elwell CE, Tyszczuk L, Cope M, Delpy DT.** Optical pathlength measurements on adult head, calf and forearm and the head of the newborn infant using phase resolved optical spectroscopy. *Phys Med Biol* 40: 295–304, 1995. doi:10.1088/0031-9155/40/2/007.
47. **Durduran T, Yodh AG.** Diffuse correlation spectroscopy for non-invasive, micro-vascular cerebral blood flow measurement. *Neuroimage* 85: 51–63, 2014. doi:10.1016/j.neuroimage.2013.06.017.
48. **Fadel PJ, Keller DM, Watanabe H, Raven PB, Thomas GD.** Noninvasive assessment of sympathetic vasoconstriction in human and rodent skeletal muscle using near-infrared spectroscopy and Doppler ultrasound. *J Appl Physiol (1985)* 96: 1323–1330, 2004. doi:10.1152/japplphysiol.01041.2003.
49. **Ferrari M, Binzoni T, Quaresima V.** Oxidative metabolism in muscle. *Philos Trans R Soc Lond B Biol Sci* 352: 677–683, 1997. doi:10.1098/rstb.1997.0049.
50. **Ferrari M, Muthalib M, Quaresima V.** The use of near-infrared spectroscopy in understanding skeletal muscle physiology: recent developments. *Philos Trans- Royal Soc, Math Phys Eng Sci* 369: 4577–4590, 2011. doi:10.1098/rsta.2011.0230.
51. **Ferrari M, Wei Q, Carraresi L, De Blasi RA, Zaccanti G.** Time-resolved spectroscopy of the human forearm. *J Photochem Photobiol B* 16: 141–153, 1992. doi:10.1016/1011-1344(92)80005-G.
52. **Ferreira LF, Harper AJ, Townsend DK, Lutjemeier BJ, Barstow TJ.** Kinetics of estimated human muscle capillary blood flow during recovery from exercise. *Exp Physiol* 90: 715–726, 2005. doi:10.1113/expphysiol.2005.030189.
53. **Ferreira LF, Hueber DM, Barstow TJ.** Effects of assuming constant optical scattering on measurements of muscle oxygenation by near-infrared spectroscopy during exercise. *J Appl Physiol (1985)* 102: 358–367, 2007. doi:10.1152/japplphysiol.00920.2005.
54. **Ferreira LF, Koga S, Barstow TJ.** Dynamics of noninvasively estimated microvascular O2 extraction during ramp exercise. *J Appl Physiol (1985)* 103: 1999–2004, 2007. doi:10.1152/japplphysiol.01414.2006.
55. **Ferreira LF, McDonough P, Behnke BJ, Musch TI, Poole DC.** Blood flow and O2 extraction as a function of O2 uptake in muscles composed of different fiber types. *Respir Physiol Neurobiol* 153: 237–249, 2006. doi:10.1016/j.resp.2005.11.004.
56. **Ferreira LF, Padilla DJ, Musch TI, Poole DC.** Temporal profile of rat skeletal muscle capillary haemodynamics during recovery from contractions. *J Physiol* 573: 787–797, 2006. doi:10.1113/jphysiol.2006.104802.
57. **Ferreira LF, Poole DC, Barstow TJ.** Muscle blood flow-O2 uptake interaction and their relation to on-exercise dynamics of O2 exchange. *Respir Physiol Neurobiol* 147: 91–103, 2005. doi:10.1016/j.resp.2005.02.002.
58. **Fick A.** *Ueber die Messung dea Blutquantums in den Herzventrikela*. Verhandlungen der Physikalisch-medizinische Gesellschaft zu Wurzburg, 1870.
59. **Fick A.** Ueber Diffusion. *Ann Phys* 170: 59–86, 1855. doi:10.1002/andp.18551700105.
60. **Flear CTG, Carpenter RG, Florence I.** Variability in water sodium potassium and chloride content of human skeletal muscle. *J Clin Pathol* 18: 74–81, 1965. doi:10.1136/jcp.18.1.74.
61. **Fontana FY, Keir DA, Bellotti C, De Roia GF, Murias JM, Pogliaghi S.** Determination of respiratory point compensation in healthy adults: Can non-invasive near-infrared spectroscopy help? *J Sci Med Sport* 18: 590–595, 2015. doi:10.1016/j.jsams.2014.07.016.
62. **Fotedar LK, Slopis JM, Narayana PA, Fenstermacher MJ, Pivarnik J, Butler IJ.** Proton magnetic resonance of exercise-induced water changes in gastrocnemius muscle. *J Appl Physiol (1985)* 69: 1695–1701, 1990. doi:10.1152/jappl.1990.69.5.1695.
63. **Franceschini MA, Boas DA, Zourabian A, Diamond SG, Nadgir S, Lin DW, Moore JB, Fantini S.** Near-infrared spiroximetry: noninvasive measurements of venous saturation in piglets and human subjects. *J Appl Physiol (1985)* 92: 372–384, 2002. doi:10.1152/jappl.2002.92.1.372.
64. **Franceschini MA, Fantini S, Paunescu LA, Maier JS, Gratton E.** Influence of a superficial layer in the quantitative spectroscopic study of strongly scattering media. *Appl Opt* 37: 7447–7458, 1998. doi:10.1364/AO.37.007447.
65. **Fujisaka SI, Ozaki T, Suzuki T, Kamada T, Kitazawa K, Nishizawa M, Takahashi A, Suzuki S.** A clinical tissue oximeter using NIR time-resolved spectroscopy. *Adv Exp Med Biol* 876: 427–433, 2016. doi:10.1007/978-1-4939-3023-4_54.
66. **Grassi B, Marzorati M, Lanfranconi F, Ferri A, Longaretti M, Stucchi A, Vago P, Marconi C, Morandi L.** Impaired oxygen extraction in metabolic myopathies: detection and quantification by near-infrared spectroscopy. *Muscle Nerve* 35: 510–520, 2007. doi:10.1002/mus.20708.
67. **Grassi B, Pogliaghi S, Rampichini S, Quaresima V, Ferrari M, Marconi C, Cerretelli P.** Muscle oxygenation and pulmonary gas exchange kinetics during cycling exercise on-transitions in humans. *J Appl Physiol (1985)* 95: 149–158, 2003. doi:10.1152/japplphysiol.00695.2002.
68. **Grassi B, Quaresima V.** Near-infrared spectroscopy and skeletal muscle oxidative function in vivo in health and disease: a review from an exercise physiology perspective. *J Biomed Opt* 21: 091313, 2016. doi:10.1117/1.JBO.21.9.091313.
69. **Grassi B, Quaresima V, Marconi C, Ferrari M, Cerretelli P.** Blood lactate accumulation and muscle deoxygenation during incremental exercise. *J Appl Physiol (1985)* 87: 348–355, 1999. doi:10.1152/jappl.1999.87.1.348.
70. **Gratton E, Fantini S, Franceschini MA, Gratton G, Fabiani M.** Measurements of scattering and absorption changes in muscle and brain. *Philos Trans R Soc Lond B Biol Sci* 352: 727–735, 1997. doi:10.1098/rstb.1997.0055.
71. **Grieger S, Geraskin D, Steimers A, Kohl-Bareis M.** Analysis of NIRS-based muscle oxygenation parameters by inclusion of adipose tissue thickness. *Adv Exp Med Biol* 789: 131–136, 2013. doi:10.1007/978-1-4614-7411-1_18.
72. **Habazettl H, Athanasopoulos D, Kuebler WM, Wagner H, Roussos C, Wagner PD, Ungruhe J, Zakynthinos S, Vogiatzis I.** Near-infrared spectroscopy and indocyanine green derived blood flow index for non-invasive measurement of muscle perfusion during exercise. *J Appl Physiol (1985)* 108: 962–967, 2010. doi:10.1152/japplphysiol.01269.2009.

Downloaded from journals.physiology.org/journal/jappl (065.021.193.086) on March 4, 2022.

73. **Hammer SM, Alexander AM, Didier KD, Smith JR, Caldwell JT, Sutterfield SL, Ade CJ, Barstow TJ.** The noninvasive simultaneous measurement of tissue oxygenation and microvascular hemodynamics during incremental handgrip exercise. *J Appl Physiol (1985)* 124: 604–614, 2018. doi:10.1152/japplphysiol.00815.2017.
74. **Harper AJ, Ferreira LF, Lutjemeier BJ, Townsend DK, Barstow TJ.** Human femoral artery and estimated muscle capillary blood flow kinetics following the onset of exercise. *Exp Physiol* 91: 661–671, 2006. doi:10.1113/expphysiol.2005.032904.
75. **Homma S, Eda H, Ogasawara S, Kagaya A.** Near-infrared estimation of O_2 supply and consumption in forearm muscles working at varying intensity. *J Appl Physiol (1985)* 80: 1279–1284, 1996. doi:10.1152/jappl.1996.80.4.1279.
76. **Homma S, Fukunaga T, Kagaya A.** Influence of adipose tissue thickness on near infrared spectroscopic signal in the measurement of human muscle. *J Biomed Opt* 1: 418–424, 1996. doi:10.1117/12.252417.
78. **Hoshi Y, Yamada Y.** Overview of diffuse optical tomography and its clinical applications. *J Biomed Opt* 21: 091312, 2016. doi:10.1117/1.JBO.21.9.091312.
79. **Hu G, Zhang Q, Ivkovic V, Strangman GE.** Ambulatory diffuse optical tomography and multimodality physiological monitoring system for muscle and exercise applications. *J Biomed Opt* 21: 091314, 2016. doi:10.1117/1.JBO.21.9.091314.
80. **Hueber DM, Franceschini MA, Ma HY, Zhang Q, Ballesteros JR, Fantini S, Wallace D, Ntziachristos V, Chance B.** Non-invasive and quantitative near-infrared haemoglobin spectrometry in the piglet brain during hypoxic stress, using a frequency-domain multidistance instrument. *Phys Med Biol* 46: 41–62, 2001. doi:10.1088/0031-9155/46/1/304.
81. **Jöbsis FF.** Noninvasive, infrared monitoring of cerebral and myocardial oxygen sufficiency and circulatory parameters. *Science* 198: 1264–1267, 1977. doi:10.1126/science.929199.
82. **Jones RH, Molitoris BA.** A statistical method for determining the breakpoint of two lines. *Anal Biochem* 141: 287–290, 1984. doi:10.1016/0003-2697(84)90458-5.
83. **Keir DA, Fontana FY, Robertson TC, Murias JM, Paterson DH, Kowalchuk JM, Pogliaghi S.** Exercise intensity thresholds: identifying the boundaries of sustainable performance. *Med Sci Sports Exerc* 47: 1932–1940, 2015. doi:10.1249/MSS.0000000000000613.
84. **Kim JG, Xia M, Liu H.** Extinction coefficients of hemoglobin for near-infrared spectroscopy of tissue. *IEEE Eng Med Biol Mag* 24: 118–121, 2005. doi:10.1109/MEMB.2005.1411359.
85. **Kindig CA, Richardson TE, Poole DC.** Skeletal muscle capillary hemodynamics from rest to contractions: implications for oxygen transfer. *J Appl Physiol (1985)* 92: 2513–2520, 2002. doi:10.1152/japplphysiol.01222.2001.
86. **Klitzman B, Duling BR.** Microvascular hematocrit and red cell flow in resting and contracting striated muscle. *Am J Physiol Heart Circ Physiol* 237: H481–H490, 1979. doi:10.1152/ajpheart.1979.237.4.H481.
87. **Koga S, Barstow TJ, Okushima D, Rossiter HB, Kondo N, Ohmae E, Poole DC.** Validation of a high-power, time-resolved, near-infrared spectroscopy system for measurement of superficial and deep muscle deoxygenation during exercise. *J Appl Physiol (1985)* 118: 1435–1442, 2015. doi:10.1152/japplphysiol.01003.2014.
88. **Koga S, Poole DC, Ferreira LF, Whipp BJ, Kondo N, Saitoh T, Ohmae E, Barstow TJ.** Spatial heterogeneity of quadriceps muscle deoxygenation kinetics during cycle exercise. *J Appl Physiol (1985)* 103: 2049–2056, 2007. doi:10.1152/japplphysiol.00627.2007.
89. **Koga S, Poole DC, Fukuoka Y, Ferreira LF, Kondo N, Ohmae E, Barstow TJ.** Methodological validation of the dynamic heterogeneity of muscle deoxygenation within the quadriceps during cycle exercise. *Am J Physiol Regul Integr Comp Physiol* 301: R534–R541, 2011. doi:10.1152/ajpregu.00101.2011.
90. **Koga S, Poole DC, Kondo N, Oue A, Ohmae E, Barstow TJ.** Effects of increased skin blood flow on muscle oxygenation/deoxygenation: comparison of time-resolved and continuous-wave near-infrared spectroscopy signals. *Eur J Appl Physiol* 115: 335–343, 2015. doi:10.1007/s00421-014-3019-2.
91. **Koga S, Shiojiri T, Kondo N, Barstow TJ.** Effect of increased muscle temperature on oxygen uptake kinetics during exercise. *J Appl Physiol (1985)* 83: 1333–1338, 1997. doi:10.1152/jappl.1997.83.4.1333.
92. **Krustrup P, González-Alonso J, Quistorff B, Bangsbo J.** Muscle heat production and anaerobic energy turnover during repeated intense dynamic exercise in humans. *J Physiol* 536: 947–956, 2001. doi:10.1111/j.1469-7793.2001.00947.x.
93. **Lai N, Zhou H, Saidel GM, Wolf M, McCully K, Gladden LB, Cabrera ME.** Modeling oxygenation in venous blood and skeletal muscle in response to exercise using near-infrared spectroscopy. *J Appl Physiol (1985)* 106: 1858–1874, 2009. doi:10.1152/japplphysiol.91102.2008.
94. **Lanfranconi F, Borrelli E, Ferri A, Porcelli S, Maccherini M, Chiavarelli M, Grassi B.** Noninvasive evaluation of skeletal muscle oxidative metabolism after heart transplant. *Med Sci Sports Exerc* 38: 1374–1383, 2006. doi:10.1249/01.mss.0000228943.62776.69.
95. **Layec G, Trinity JD, Hart CR, Kim SE, Groot HJ, Le Fur Y, Sorensen JR, Jeong EK, Richardson RS.** In vivo evidence of an age-related increase in ATP cost of contraction in the plantar flexor muscles. *Clin Sci (Lond)* 126: 581–592, 2014. doi:10.1042/CS20130442.
96. **Lima A, van Bommel J, Sikorska K, van Genderen M, Klijn E, Lesaffre E, Ince C, Bakker J.** The relation of near-infrared spectroscopy with changes in peripheral circulation in critically ill patients. *Crit Care Med* 39: 1649–1654, 2011. doi:10.1097/CCM.0b013e3182186675.
97. **Lucero AA, Addae G, Lawrence W, Neway B, Credeur DP, Faulkner J, Rowlands D, Stoner L.** Reliability of muscle blood flow and oxygen consumption response from exercise using near-infrared spectroscopy. *Exp Physiol* 103: 90–100, 2018. doi:10.1113/EP086537.
98. **Mancini DM, Bolinger L, Li H, Kendrick K, Chance B, Wilson JR.** Validation of near-infrared spectroscopy in humans. *J Appl Physiol (1985)* 77: 2740–2747, 1994. doi:10.1152/jappl.1994.77.6.2740.
99. **Marcinek DJ, Amara CE, Matz K, Conley KE, Schenkman KA.** Wavelength shift analysis: a simple method to determine the contribution of hemoglobin and myoglobin to in vivo optical spectra. *Appl Spectrosc* 61: 665–669, 2007. doi:10.1366/000370207781269819.
100. **Martin DS, Levett DZ, Bezemer R, Montgomery HE, Grocott MP; Caudwell Xtreme Everest Research Group.** The use of skeletal muscle near infrared spectroscopy and a vascular occlusion test at high altitude. *High Alt Med Biol* 14: 256–262, 2013. doi:10.1089/ham.2012.1109.
101. **McCully KK, Hamaoka T.** Near-infrared spectroscopy: what can it tell us about oxygen saturation in skeletal muscle? *Exerc Sport Sci Rev* 28: 123–127, 2000.
102. **McCully KK, Landsberg L, Suarez M, Hofmann M, Posner JD.** Identification of peripheral vascular disease in elderly subjects using optical spectroscopy. *J Gerontol A Biol Sci Med Sci* 52: B159–B165, 1997. doi:10.1093/gerona/52A.3.B159.
103. **McLay KM, Fontana FY, Nederveen JP, Guida FF, Paterson DH, Pogliaghi S, Murias JM.** Vascular responsiveness determined by near-infrared spectroscopy measures of oxygen saturation. *Exp Physiol* 101: 34–40, 2016. doi:10.1113/EP085406.
104. **McLay KM, Gilbertson JE, Pogliaghi S, Paterson DH, Murias JM.** Vascular responsiveness measured by tissue oxygen saturation reperfusion slope is sensitive to different occlusion durations and training status. *Exp Physiol* 101: 1309–1318, 2016. doi:10.1113/EP085843.
105. **Messere A, Roatta S.** Influence of cutaneous and muscular circulation on spatially resolved versus standard Beer-Lambert near-infrared spectroscopy. *Physiol Rep* 1: e00179, 2013. doi:10.1002/phy2.179.
106. **Mezzani A, Grassi B, Jones AM, Giordano A, Corrà U, Porcelli S, Della Bella S, Taddeo A, Giannuzzi P.** Speeding of pulmonary VO2 on-kinetics by light-to-moderate-intensity aerobic exercise training in chronic heart failure: clinical and pathophysiological correlates. *Int J Cardiol* 167: 2189–2195, 2013. doi:10.1016/j.ijcard.2012.05.124.
107. **Miura H, McCully K, Hong L, Nioka S, Chance B.** Regional difference of muscle oxygen saturation and blood volume during exercise determined by near infrared imaging device. *Jpn J Physiol* 51: 599–606, 2001. doi:10.2170/jjphysiol.51.599.
108. **Mizuno M, Tokizawa K, Iwakawa T, Muraoka I.** Inflection points of cardiovascular responses and oxygenation are correlated in the distal but not the proximal portions of muscle during incremental exercise. *J Appl Physiol (1985)* 97: 867–873, 2004. doi:10.1152/japplphysiol.00213.2004.
109. **Murias JM, Kowalchuk JM, Paterson DH.** Speeding of VO2 kinetics with endurance training in old and young men is associated with improved matching of local O2 delivery to muscle O2 utilization. *J Appl Physiol (1985)* 108: 913–922, 2010. doi:10.1152/japplphysiol.01355.2009.
110. **Murias JM, Spencer MD, Delorey DS, Gurd BJ, Kowalchuk JM, Paterson DH.** Speeding of VO2 kinetics during moderate-intensity exercise subsequent to heavy-intensity exercise is associated with improved local O2 distribution. *J Appl Physiol (1985)* 111: 1410–1415, 2011. doi:10.1152/japplphysiol.00607.2011.
111. **Murias JM, Spencer MD, Kowalchuk JM, Paterson DH.** Muscle deoxygenation to VO_2 relationship differs in young subjects with varying

Downloaded from journals.physiology.org/journal/jappl (065.021.193.086) on March 4, 2022.

τVO_2. *Eur J Appl Physiol* 111: 3107–3118, 2011. doi:10.1007/s00421-011-1937-9.

112. **Murias JM, Spencer MD, Pogliaghi S, Paterson DH.** Noninvasive estimation of microvascular O2 provision during exercise on-transients in healthy young males. *Am J Physiol Regul Integr Comp Physiol* 303: R815–R823, 2012. doi:10.1152/ajpregu.00306.2012.
113. **Nemeth PM, Lowry OH.** Myoglobin levels in individual human skeletal muscle fibers of different types. *J Histochem Cytochem* 32: 1211–1216, 1984. doi:10.1177/32.11.6491255.
114. **Oda M, Yamashita Y, Nakano T, Suzuki A, Shimizu K, Hirano I, Shimomura F, Ohmae E, Suzuki T, Tsuchiya Y.** Near-infrared time-resolved spectroscopy system for tissue oxygenation monitor. *Proc SPIE* 3597: 611–617, 1999. doi:10.1117/12.356809.
115. **Ohmae E, Ouchi Y, Oda M, Suzuki T, Nobesawa S, Kanno T, Yoshikawa E, Futatsubashi M, Ueda Y, Okada H, Yamashita Y.** Cerebral hemodynamics evaluation by near-infrared time-resolved spectroscopy: correlation with simultaneous positron emission tomography measurements. *Neuroimage* 29: 697–705, 2006. doi:10.1016/j.neuroimage.2005.08.008.
116. **Okushima D, Poole DC, Rossiter HB, Barstow TJ, Kondo N, Ohmae E, Koga S.** Muscle deoxygenation in the quadriceps during ramp incremental cycling: Deep vs. superficial heterogeneity. *J Appl Physiol (1985)* 119: 1313–1319, 2015. doi:10.1152/japplphysiol.00574.2015.
117. **Payen D, Luengo C, Heyer L, Resche-Rigon M, Kerever S, Damoisel C, Losser MR.** Is thenar tissue hemoglobin oxygen saturation in septic shock related to macrohemodynamic variables and outcome? *Crit Care* 13, *Suppl* 5: S6, 2009. doi:10.1186/cc8004.
118. **Perrey S, Ferrari M.** Muscle oximetry in sports science: a systematic review. *Sports Med* 48: 597–616, 2018. doi:10.1007/s40279-017-0820-1.
119. **Poole DC, Wagner PD, Wilson DF.** Diaphragm microvascular plasma PO2 measured in vivo. *J Appl Physiol (1985)* 79: 2050–2057, 1995. doi:10.1152/jappl.1995.79.6.2050.
120. **Porcelli S, Marzorati M, Lanfranconi F, Vago P, Pisot R, Grassi B.** Role of skeletal muscles impairment and brain oxygenation in limiting oxidative metabolism during exercise after bed rest. *J Appl Physiol (1985)* 109: 101–111, 2010. doi:10.1152/japplphysiol.00782.2009.
121. **Re R, Pirovano I, Contini D, Spinelli L, Torricelli A.** Time Domain Near Infrared Spectroscopy Device for Monitoring Muscle Oxidative Metabolism: Custom Probe and In Vivo Applications. *Sensors (Basel)* 18: 264, 2018. doi:10.3390/s18010264.
122. **Rendell M, Hovelson C, O'Connor K, Cheung L, Huard S, Kong TS, Catania A, Rosenthal R.** Determination of blood flow in the finger using near-infrared spectroscopy. *Clin Physiol* 18: 426–434, 1998. doi:10.1046/j.1365-2281.1998.00108.x.
123. **Rolfe P.** In vivo near-infrared spectroscopy. *Annu Rev Biomed Eng* 2: 715–754, 2000. doi:10.1146/annurev.bioeng.2.1.715.
124. **Ryan TE, Brizendine JT, Backus D, McCully KK.** Electrically induced resistance training in individuals with motor complete spinal cord injury. *Arch Phys Med Rehabil* 94: 2166–2173, 2013. doi:10.1016/j.apmr.2013.06.016.
125. **Ryan TE, Brophy P, Lin CT, Hickner RC, Neufer PD.** Assessment of in vivo skeletal muscle mitochondrial respiratory capacity in humans by near-infrared spectroscopy: a comparison with in situ measurements. *J Physiol* 592: 3231–3241, 2014. doi:10.1113/jphysiol.2014.274456.
126. **Ryan TE, Erickson ML, Brizendine JT, Young HJ, McCully KK.** Noninvasive evaluation of skeletal muscle mitochondrial capacity with near-infrared spectroscopy: correcting for blood volume changes. *J Appl Physiol (1985)* 113: 175–183, 2012. doi:10.1152/japplphysiol.00319.2012.
127. **Ryan TE, Erickson ML, Verma A, Chavez J, Rivner MH, Mccully KK.** Skeletal muscle oxidative capacity in amyotrophic lateral sclerosis. *Muscle Nerve* 50: 767–774, 2014. doi:10.1002/mus.24223.
128. **Ryan TE, Southern WM, Reynolds MA, McCully KK.** A cross-validation of near-infrared spectroscopy measurements of skeletal muscle oxidative capacity with phosphorus magnetic resonance spectroscopy. *J Appl Physiol (1985)* 115: 1757–1766, 2013. doi:10.1152/japplphysiol.00835.2013.
129. **Scholkmann F, Kleiser S, Metz AJ, Zimmermann R, Mata Pavia J, Wolf U, Wolf M.** A review on continuous wave functional near-infrared spectroscopy and imaging instrumentation and methodology. *Neuroimage* 85: 6–27, 2014. doi:10.1016/j.neuroimage.2013.05.004.
130. **Seiyama A, Hazeki O, Tamura M.** Noninvasive quantitative analysis of blood oxygenation in rat skeletal muscle. *J Biochem* 103: 419–424, 1988. doi:10.1093/oxfordjournals.jbchem.a122285.
131. **Southern WM, Ryan TE, Kepple K, Murrow JR, Nilsson KR, McCully KK.** Reduced skeletal muscle oxidative capacity and impaired training adaptations in heart failure. *Physiol Rep* 3: e12353, 2015. doi:10.14814/phy2.12353.
132. **Southern WM, Ryan TE, Reynolds MA, McCully K.** Reproducibility of near-infrared spectroscopy measurements of oxidative function and postexercise recovery kinetics in the medial gastrocnemius muscle. *Appl Physiol Nutr Metab* 39: 521–529, 2014. doi:10.1139/apnm-2013-0347.
133. **Stolik S, Delgado JA, Pérez A, Anasagasti L.** Measurement of the penetration depths of red and near infrared light in human "ex vivo" tissues. *J Photochem Photobiol B* 57: 90–93, 2000. doi:10.1016/S1011-1344(00)00082-8.
134. **Suzuki S, Takasaki S, Ozaki T, Kobayashi Y.** A tissue oxygenation monitor using NIR spatially resolved spectroscopy. *Proc SPIE* 3597: 582–592, 1999. doi:10.1117/12.356862.
135. **Torricelli A, Contini D, Pifferi A, Caffini M, Re R, Zucchelli L, Spinelli L.** Time domain functional NIRS imaging for human brain mapping. *Neuroimage* 85: 28–50, 2014. doi:10.1016/j.neuroimage.2013.05.106.
136. **Tran TK, Sailasuta N, Kreutzer U, Hurd R, Chung Y, Mole P, Kuno S, Jue T.** Comparative analysis of NMR and NIRS measurements of intracellular PO2 in human skeletal muscle. *Am J Physiol Regul Integr Comp Physiol* 276: R1682–R1690, 1999. doi:10.1152/ajpregu.1999.276.6.R1682.
137. **Tschakovsky ME, Shoemaker JK, Hughson RL.** Beat-by-beat forearm blood flow with Doppler ultrasound and strain-gauge plethysmography. *J Appl Physiol (1985)* 79: 713–719, 1995. doi:10.1152/jappl.1995.79.3.713.
138. **van Beek-Harmsen BJ, Bekedam MA, Feenstra HM, Visser FC, van der Laarse WJ.** Determination of myoglobin concentration and oxidative capacity in cryostat sections of human and rat skeletal muscle fibres and rat cardiomyocytes. *Histochem Cell Biol* 121: 335–342, 2004. doi:10.1007/s00418-004-0641-9.
139. **van Beekvelt MC, Borghuis MS, van Engelen BG, Wevers RA, Colier WN.** Adipose tissue thickness affects in vivo quantitative near-IR spectroscopy in human skeletal muscle. *Clin Sci (Lond)* 101: 21–28, 2001. doi:10.1042/cs1010021.
140. **van Beekvelt MC, van Engelen BG, Wevers RA, Colier WN.** In vivo quantitative near-infrared spectroscopy in skeletal muscle during incremental isometric handgrip exercise. *Clin Physiol Funct Imaging* 22: 210–217, 2002. doi:10.1046/j.1475-097X.2002.00420.x.
141. **van Beekvelt MCP, Colier WNJM, Wevers RA, van Engelen BGM.** Performance of near-infrared spectroscopy in measuring local O(2) consumption and blood flow in skeletal muscle. *J Appl Physiol (1985)* 90: 511–519, 2001. doi:10.1152/jappl.2001.90.2.511.
142. **Wang L, Yoshikawa T, Hara T, Nakao H, Suzuki T, Fujimoto S.** Which common NIRS variable reflects muscle estimated lactate threshold most closely? *Appl Physiol Nutr Metab* 31: 612–620, 2006. doi:10.1139/h06-069.
143. **Wassenaar EB, Van den Brand JG.** Reliability of near-infrared spectroscopy in people with dark skin pigmentation. *J Clin Monit Comput* 19: 195–199, 2005. doi:10.1007/s10877-005-1655-0.
144. **Watzman HM, Kurth CD, Montenegro LM, Rome J, Steven JM, Nicolson SC.** Arterial and venous contributions to near-infrared cerebral oximetry. *Anesthesiology* 93: 947–953, 2000. doi:10.1097/00000542-200010000-00012.
145. **Willingham TB, McCully KK.** *In vivo* assessment of mitochondrial dysfunction in clinical populations using near-infrared spectroscopy. *Front Physiol* 8: 689, 2017. doi:10.3389/fphys.2017.00689.
146. **Wolf U, Wolf M, Choi JH, Paunescu LA, Michalos A, Gratton E.** Regional differences of hemodynamics and oxygenation in the human calf muscle detected with near-infrared spectrophotometry. *J Vasc Interv Radiol* 18: 1094–1101, 2007. doi:10.1016/j.jvir.2007.06.004.
147. **Wray S, Cope M, Delpy DT, Wyatt JS, Reynolds EO.** Characterization of the near infrared absorption spectra of cytochrome aa3 and haemoglobin for the non-invasive monitoring of cerebral oxygenation. *Biochim Biophys Acta* 933: 184–192, 1988. doi:10.1016/0005-2728(88)90069-2.
148. **Zonios G, Bykowski J, Kollias N.** Skin melanin, hemoglobin, and light scattering properties can be quantitatively assessed in vivo using diffuse reflectance spectroscopy. *J Invest Dermatol* 117: 1452–1457, 2001. doi:10.1046/j.0022-202x.2001.01577.x.

Downloaded from journals.physiology.org/journal/jappl (065.021.193.086) on March 4, 2022.